Numerical analysis of mixed mode (I/II) stress intensity factors of single edge cracked/notched plates under different boundary conditions using strain energy approach

Liang Shi
University of Manchester
S Olutunde Oyadiji (s.o.oyadiji@manchester.ac.uk)
University of Manchester

Research Article

Keywords: slant crack/notch, mode I/II, stress intensity factors, finite element analysis, strain energy approach

Posted Date: September 22nd, 2022

DOI: https://doi.org/10.21203/rs.3.rs-2061136/v1

Numerical analysis of mixed mode (I/II) stress intensity factors of single edge cracked/notched plates under different boundary conditions using strain energy approach

Liang Shi, S Olutunde Oyadiji
Department of Mechanical, Aerospace and Civil Engineering,
University of Manchester, Manchester M13 9PL, UK

Abstract

The stress intensity factor is a conventional parameter in Fracture Mechanics and there are some analytical solutions for many different fracture cases. This paper presents the mixed mode I/II stress intensity factors (SIF) of slanted cracks/notches under tension loading. A two-dimensional finite element analysis was employed using ABAQUS finite element program. Various crack lengths and angles were analysed. The effect of the different boundary conditions applied at the plate edge was also examined. Based on the literature survey, there is a lack of solution of SIFs of slanted cracks in plane stress plates. The strain energy approach (SEA) was adopted to analyse the notched cases since finite element software are not capable of computing the notched SIFs directly. By obtaining the strain energy in the FEA results, mode I and II SIFs can be calculated simply by using the SEA method. Moreover, the accuracy of this approach has been validated and compared with the available published results and shows an excellent agreement. The key contribution of the present paper is to evaluate the effect of the crack/notch length to plate width ratio on the mode I and II SIFs of a slant-edge-cracked/notched plate under different boundary conditions, i.e. pinned boundary condition and clamped boundary condition. Crack/notch length to plate width ratios from 0.1 to 0.9, slant angle from 0º to 45º, notch initial angle from 0º to 45º were considered. Series of new data of mode I and II SIFs are provided herein.

Key words: slant crack/notch, mode I/II, stress intensity factors, finite element analysis, strain energy approach

1. Introduction

With the huge development of engineering structures, and especially of built-up welded structures, such as ships, aircraft, building frames, bridge decks, oil refineries and offshore oil platforms, cracks/notches may exist in any part of the structures under complex loading conditions. Thus, it is necessary to study crack initiation and propagation. The study of mixed mode fracture criterion and crack propagation has become of great significance in Fracture Mechanics and Engineering. Much work has been carried out in this area and some criteria have been established to predict crack initiation angle and critical fracture

load of materials that lead to mixed mode I / II fracture at the crack tip under loading. The stress intensity factor (SIF) at the crack tip is an important parameter for predicting the failure state of a structure. Therefore, several approaches have been proposed to predict the stress intensity factor (SIF), which can be used to establish failure criteria for a structure. These criteria can be classified according to the key parameters that define the criteria and these parameters may be critical values for stress, strain or energy.

In the literature, there is a much greater focus and emphasis on computing the stress intensity factors of cracks in structures such as cracked plates. However, most cracks in structures are initiated from microscopic notches which may be due to machining imperfections, material imperfections and/or dents caused by objects impacting the structure. Also, in the controlled experimental studies of cracked structures, notches are often created on the structure to serve as sites for the initiation of cracks from which crack growth and propagation occur. Therefore, the study of SIFs at notch tips is also very important as the notch tip SIFs control the initiation, growth and propagation of cracks. Consequently, mixed mode SIFs of both cracked and notched plates are considered in this paper. Furthermore, the magnitudes of the SIFs are controlled by the boundary conditions of the structure. In most cases, the SIFs of cracked structures are computed under pinned-pinned boundary conditions. This gives a conservative overestimate of the SIFs and leads to an overdesign of a structure. In the aerospace and space engineering fields, such conservative design leads to relatively heavier structures. For light weight design, it is essential to consider clamped-clamped boundary conditions which are closer representations of the boundary conditions of an actual cracked/notched structure. This will enable determination of the additional weight due to the conservative design and may provoke novel designs to strengthen highly stressed regions whilst minimising additional weight.

Erdogan and Shi [1] were the first to propose a crack initiation criterion using the stress as a critical parameter which was called the maximum tangential stress (MTS) criterion. In order to support this criterion, Erdogan and Shi [1] used brittle plexiglas plates to carry out experiments to validate that the MTS criterion was available to analyse brittle materials. Later, through re-examining and modifying the Griffith concept [2], Sih and Macdonald [3-5] proposed a new concept of minimum strain energy density $\boldsymbol{S}$ criterion using a critical parameter of strain. In addition, this $\boldsymbol{S}$ criterion is capable of predicting the crack growth direction subjected to mixed mode I/II conditions. On the other hand, Hussain et al. [6] used the maximum energy release rate criterion on a crack subjected to mode I and mode II conditions and the theory has been validated via experimental test results.

Based on the strain field around the crack tip, Theocaris et al. [7-9] introduced a new fracture criterion of maximum dilatational strain energy ($\boldsymbol{T}$) criterion. They applied the $\boldsymbol{T}$ criterion on polycarbonate of bisphenol A (PCBA) specimens and the theoretical predictions were in good agreement with the experimental results. Similarly, with using the stress as a critical parameter, Kong et al. [10] developed the maximum triaxial stress ($\boldsymbol{M}$) criterion. Kong et al.'s [10] experimental results were consistent with

the results from theoretical analysis as well as the experimental results by Theocaris et al. [7-9]. Later, Lazzarin et al. [11-18] carried out many researches on theoretical analysis of strain energy density (SED) for V- and blunt U-notches in plates under mode I, mode II or mixed mode loading. On the other hand, based on the strain energy of a control volume in the notch tip region, Treifi and Oyadiji (2013) developed a strain energy approach (SEA) to compute the general SIFs for V-notched plates under mode I, II and III loading conditions [19]. The formulae in the SEA are simple and easy to implement. The strain energy around the notch tip regions can be easily computed using finite element packages and then the notch SIFs can be calculated. However, the commercial finite element packages (ABAQUS, ANSYS, FRANC2D) are not generally capable of computing the SIFs of a notch directly; they are only able to compute the SIFs of a crack directly.

Determination of fracture parameters, such as stress intensity factor (SIF) and strain energy release rate by finite element analysis requires either generating a refined mesh around the crack tip or employing special elements to arrest the stress singularity near the crack tip. In order to capture the stress behaviour at the crack tip [20-22], it is necessary to apply very small elements near the crack tip conventionally, and it is likely to underestimate the sharply rising stress-displacement gradient. To avoid these problems, Hanshell and Shaw [23] and Barsoum [24, 25] proposed a special element to correctly capture the crack tip singularity. The mid-side nodes of 8-node isoparametric quadrilateral elements are shifted to the one quarter point from the crack tip node, which achieves the desired $1/\sqrt{r}$ singular behaviour. By the Finite Element Method (FEM), Petit et al. [26] obtained the displacement field to determine the SIFs (K_I and K_{II}) under mixed mode I/II conditions and investigated the crack propagation for an oblique edge-cracked panel with crack angle of 45º. Later, Hedayati and Vahedi [27] evaluated the SIFs and crack propagation direction of a slanted-crack plate using Extended Finite Element Method (XFEM) and conventional Finite Element Method (FEM) in the ABAQUS software and the numerical results were in good agreement with the theoretical predictions.

However, the problem of slant edge cracks/notches offset from the middle of the plate edge, which cannot be analysed theoretically, has not been widely analysed by the Finite Element Analysis (FEA) technique because the commercial FEA software packages cannot compute the SIFs of notched structures directly. Therefore, the main objective of the current work is to use the strain energy approach (SEA) to quantify the effects of edge crack/notch positions on the mixed mode I and II SIFs of open cracks/notches. The ABAQUS FEA code is utilized to perform a mixed-mode finite element analysis of plates with slant edge cracks/notches subjected to uniaxial loading. The predicted strain energies of the elements around the crack/notch tips are used to compute the mixed mod I/II SIFs of the cracked/notched plates using the procedures described in section 3 of the paper. Mixed mode I/II SIFs (K_I and K_{II}) were determined in terms of three parameters, namely: the length of the crack/notch, the inclination angle of the crack/notch and the initial angle of the notch. It is obvious that the crack problem can be regarded as zero-angle notch problem. The accuracy of this approach is evaluated by some

examples under uniaxial loading conditions. It is shown that the computed mixed mode I/II SIFs manifest excellent agreement with the available published results. In addition, both the pinned-pinned and clamped-clamped boundary conditions are applied to the single edge cracked/notched plates and new SIF (K_I and K_{II}) results are presented.

2. Computations mixed mode I/II SIFs for cracked plates using conventional Finite Element Method

Slant single edge-crack/notch plate under tensile loading was analysed under different boundary conditions. The finite element code ABAQUS/CAE 2018 was utilized to analyse a full model of the slant single edge-crack/notch plate. To investigate the mix modes I/II fracture behaviour of the crack/notch, the present model was achieved under plane stress conditions. The plate was described in Fig. 1: the height (H) was 200 mm and the width (W) was 100 mm. The crack/notch height was fixed as, $h = H/2$. The crack/notch length (a) to the plate width (W) ratios, a/W, increase from 0.1 to 0.9 with a step of 0.1. The slant angle of the crack/notch, β, ranges from 0º to 45º with an increment of 5º anticlockwise. The notch initial angle, γ, increases from 0º to 45º with an increment of 5º and it is noted that a crack can be regarded specially as a zero initial angle notch. An isotropic material was adopted for the model with the Young's modulus of E = 200GPa and the Poisson's ratio of v = 0.3. As recommended in ABAQUS User's Manual [28], the eight node plane stress element, CPS8, with full integration was adopted in the numerical model, which was able to address the stress gradients successfully.

The slant single edge-crack/notch plate was loaded with a uniform tensile (axial) stress which was applied at the top and bottom edges of the plate. In order to investigate how the boundary conditions influence the singularity behaviour of the crack/notch tip region, two different boundary conditions of pinned ends and clamped ends are applied on the plate. For the pinned boundary conditions, the tensile stress is applied to the top and bottom edges of the plate. However, to achieve the clamped boundary conditions, a top-right corner node was restricted with fixed translation along x-direction and fixed rotation about z-direction, that is Ux=0 and URz=0, and then the top edge was kinematic coupled with the top-right corner node. Similarly, the bottom edge and the bottom-right corner node are restricted similarly as in the previous step.

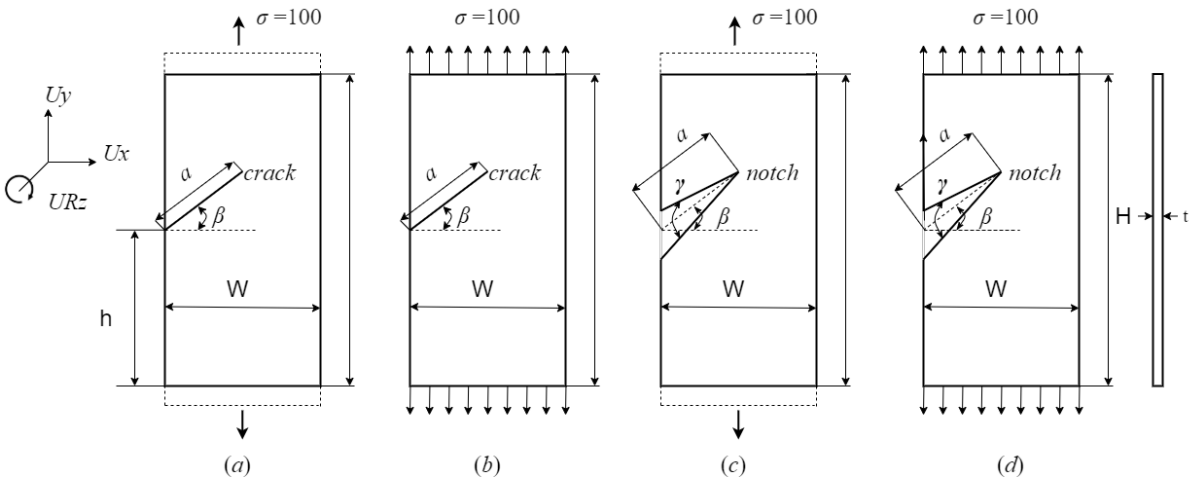

Fig. 1 . Typical numerical model sketch; (a) Slant edge-crack plate with pinned ends; (b) Slant edge-crack plate with clamped ends; (c) Slant edge-notch plate with pinned ends; (d) Slant edge-notch plate with clamped ends;

The plate was subjected to a uniform tensile loading, σ = 100 Pa, applied at its top and bottom edges, as shown in Fig. 1 and the pinned boundary conditions and clamped boundary conditions are shown as well. To correctly address the singularity behaviour [23-25], the quarter-point elements are applied to model the crack tip region, as shown in Fig. 2.

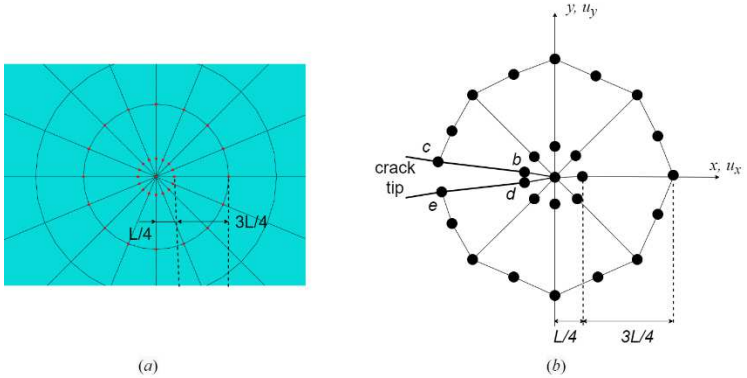

Fig. 2. (a) A part mesh of crack tip region; (b) Quarter-point element sketch at crack tip

By using the finite element code ABAQUS, the dimensional stress intensity factors K_I and K_{II} can be obtained from the finite element analysis. The normalized stress intensity factors was calculated by the following formulae:

$$\kappa_I = K_I/\sigma\sqrt{\pi a} \quad (1)$$

$$\kappa_{II} = K_{II}/\sigma\sqrt{\pi a} \quad (2)$$

where K_I and K_{II} are mode I and mode II stress intensity factor, respectively, a is crack length and σ is the applied tensile stress. It is noted that these formulae are only used for cracked cases as the commercial finite element packages are not generally capable of computing the SIFs of a notch directly.

The SIFs (K_I and K_{II}) for the notched cases are calculated using strain energy approach, as presented below.

3. Strain energy approach (SEA) for SIFs evaluation of V-notch problems

The strain energy of a finite volume around a notch tip can be described as [29]:

$$E^{(e)} = \int_v W^{(e)}\, dV \tag{3}$$

where $W^{(e)}$ is the strain energy density and is defined as:

$$W^{(e)} = \int \sigma : \partial\varepsilon \tag{4}$$

where σ and ε are stress and strain tensors, respectively. For an isotropic material, the strain energy density $W^{(e)}$ for a generalised state of stress can be described as:

$$W^{(e)} = \frac{1}{2}\left[\sigma_{xx}\varepsilon_{xx} + \sigma_{yy}\varepsilon_{yy} + \sigma_{zz}\varepsilon_{zz} + \tau_{xy}\gamma_{xy} + \tau_{xz}\gamma_{xz} + \tau_{yz}\gamma_{yz}\right] \tag{5}$$

In terms of the stresses using Hooke's law, the strains can be written as:

$$\varepsilon_{xx} = \frac{1}{E}\left[\sigma_{xx} - v\left(\sigma_{yy} + \sigma_{zz}\right)\right] \tag{6}$$

$$\varepsilon_{yy} = \frac{1}{E}\left[\sigma_{yy} - v(\sigma_{xx} + \sigma_{zz})\right] \tag{7}$$

$$\varepsilon_{zz} = \frac{1}{E}\left[\sigma_{zz} - v\left(\sigma_{xx} + \sigma_{yy}\right)\right] \tag{8}$$

$$\gamma_{xy} = \frac{1}{G}\tau_{xy} \tag{9}$$

$$\gamma_{yz} = \frac{1}{G}\tau_{yz} \tag{10}$$

$$\gamma_{xz} = \frac{1}{G}\tau_{xz} \tag{11}$$

where E is the Young's modulus, v is the Possion's ratio and $G = \frac{E}{2(1+v)}$ is the shear modulus. For simplicity, the stresses associated with different modes of deformation I, II and III can be expressed as:

$$\sigma_{ij} = f(K_I, K_{II}, K_{III}, r, \theta);\ \ i = x, y, z;\ \ j = x, y, z. \tag{12}$$

where $K_I, K_{II}\ and\ K_{III}$ are the mode I, II and III SIFs, respectively. By submitting the stress expressions into Eq. (3) and carrying out the integration over a finite volume around the notch tip, Eq. (3) becomes a representation of a direct relation between the strain energy for a finite volume and the SIFs. Thus, this approach is quite useful to extract SIFs for general notches from results of computations carried out using finite element packages.

3.1 Relationships between SIFs and strain energy around a notch tip under in-plane loading conditions (mode I, II and mixes mode)

For the in-plane problem, the strain energy density is

$$W^{(e)} = \frac{1}{2E}\left[{\sigma_{xx}}^2 + {\sigma_{yy}}^2 + {\sigma_{zz}}^2 - 2v(\sigma_{xx}\sigma_{xx} + \sigma_{yy}\sigma_{yy} + \sigma_{zz}\sigma_{zz}) + 2(1+v){\tau_{xy}}^2\right] \tag{13}$$

where $\sigma_{zz} = 0$ for plane-stress problem and $\sigma_{zz} = v(\sigma_{xx} + \sigma_{yy})$ for plane-strain problem.

For a given angular co-ordinate θ in Fig. 3(a) there is an infinite set of eigenvalues, λ_n^I for mode I and λ_n^{II} for mode II, and a corresponding infinite set of eigenvectors, the stress distributions can be written as [30, 31]:

$$\begin{aligned}\sigma_{xx} = \sum_{n=1}^{\infty} Re\Big\{ & \lambda_n^I r^{\lambda_n^I - 1} A_1[(2 + \lambda_n^I cos2\alpha + cos2\lambda_n^I\alpha)\cos(\lambda_n^I - 1)\,\theta \\ & - (\lambda_n^I - 1)\cos(\lambda_n^I - 3)\,\theta] \\ & + \lambda_n^{II} r^{\lambda_n^{II} - 1} A_2[-(2 + \lambda_n^{II}\cos2\alpha - \cos2\lambda_n^{II}\alpha)\sin(\lambda_n^{II} - 1)\,\theta + (\lambda_n^{II} \\ & - 1)\sin(\lambda_n^{II} - 3)\theta]\Big\}\end{aligned} \tag{14}$$

$$\begin{aligned}\sigma_{yy} = \sum_{n=1}^{\infty} Re\Big\{ & \lambda_n^I r^{\lambda_n^I - 1} A_1[(2 - \lambda_n^I cos2\alpha - cos2\lambda_n^I\alpha)\cos(\lambda_n^I - 1)\,\theta \\ & - (\lambda_n^I - 1)\cos(\lambda_n^I - 3)\,\theta] \\ & + \lambda_n^{II} r^{\lambda_n^{II} - 1} A_2[(-2 + \lambda_n^{II} cos2\alpha - cos2\lambda_n^{II}\alpha)\sin(\lambda_n^{II} - 1)\,\theta - (\lambda_n^{II} \\ & - 1)\sin(\lambda_n^{II} - 3)\theta]\Big\}\end{aligned} \tag{15}$$

$$\begin{aligned}\tau_{xy} = \sum_{n=1}^{\infty} Re\Big\{ & \lambda_n^I r^{\lambda_n^I - 1} A_1[-(\lambda_n^I cos2\alpha + cos2\lambda^I\alpha)\sin(\lambda_n^I - 1)\,\theta + (\lambda_n^I - 1)\sin(\lambda_n^I \\ & - 3)\theta] + \lambda_n^{II} r^{\lambda_n^{II} - 1} A_2[-(\lambda_n^{II} cos2\alpha - cos2\lambda_n^{II}\alpha)\cos(\lambda_n^{II} - 1)\,\theta + (\lambda_n^{II} \\ & - 1)\cos(\lambda_n^{II} - 3)\theta]\Big\}\end{aligned} \tag{16}$$

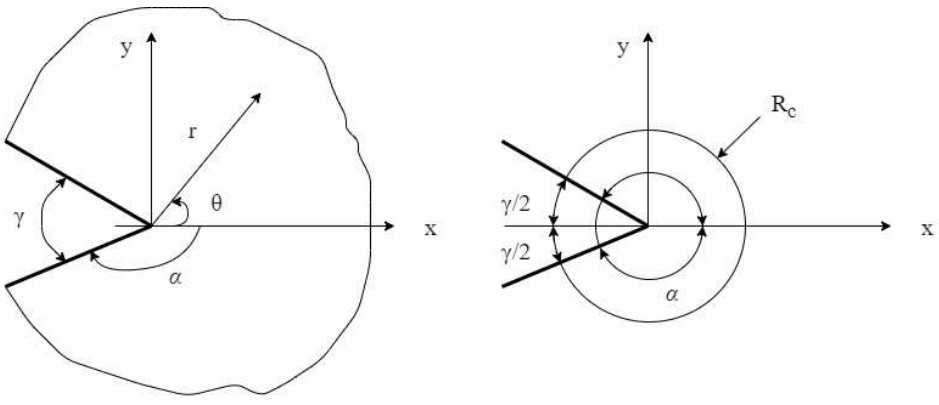

Fig. 3. (a) Isotropic homogeneous notch geometry; (b) Integral domain.

where λ^I and λ^{II} are eigenvalues and can be calculated by using the following characteristic equations:

$$\lambda^I sin2\alpha + sin2\lambda^I\alpha = 0 \tag{17}$$

$$\lambda^{II} sin2\alpha - sin2\lambda^{II}\alpha = 0 \tag{18}$$

A_1 and A_2 are constants related to the mode I and mode II SIFs

$$K_I = \sqrt{2\pi}\lambda^I(1 + \lambda^I - \lambda^I cos2\alpha - cos2\lambda^I\alpha)A_1 \tag{19}$$

$$K_{II} = \sqrt{2\pi}\lambda^{II}(-1 + \lambda^{II} - \lambda^{II} cos2\alpha + cos2\lambda^{II}\alpha)A_2 \tag{20}$$

Eqs. (14)-(16) are eigenfunction series expansions. It should be noted that only the singular terms are considered in the SEA. In order to facilitate the analysis and explanation of the problem, the stress expressions of Eqs. (14)-(16) can be rewritten as:

$$\sigma_{xx} = A_1 r^{\lambda^I-1} f_x(\theta) + A_2 r^{\lambda^{II}-1} \mathrm{g}_x(\theta) = A_1 r^{\lambda^I-1} f_x + A_2 r^{\lambda^{II}-1} \mathrm{g}_x \tag{21}$$

$$\sigma_{yy} = A_1 r^{\lambda^I-1} f_y(\theta) + A_2 r^{\lambda^{II}-1} \mathrm{g}_y(\theta) = A_1 r^{\lambda^I-1} f_y + A_2 r^{\lambda^{II}-1} \mathrm{g}_y \tag{22}$$

$$\tau_{xy} = A_1 r^{\lambda^I-1} f_{xy}(\theta) + A_2 r^{\lambda^{II}-1} \mathrm{g}_{xy}(\theta) = A_1 r^{\lambda^I-1} f_{xy} + A_2 r^{\lambda^{II}-1} \mathrm{g}_{xy} \tag{23}$$

where $f_x, f_y, \mathrm{g}_x, \mathrm{g}_y, f_{xy}\ and\ \mathrm{g}_{xy}$ are functions of θ; $r\ and\ \theta$ are the polar coordinates with the origin located at the notch-tip as defined in Fig. 3;

Subjected to plane-stress condition, substituting Eqs. (21)-(23) into Eq. (5) gives:

$$\begin{aligned} W^{(e)} = \frac{1}{2E}[&A_1^2 r^{2(\lambda^I-1)}(f_x^2 + f_y^2 - 2v f_x f_y + 2(1+v) f_{xy}^2 \\ &+ A_2^2 r^{2(\lambda^{II}-1)}\left(\mathrm{g}_x^2 + \mathrm{g}_y^2 - 2v\mathrm{g}_x\mathrm{g}_y + 2(1+v)\mathrm{g}_{xy}^2\right) \\ &+ A_1 A_2 r^{(\lambda^I+\lambda^{II}-2)}(2f_x\mathrm{g}_x + 2f_y\mathrm{g}_y - 2v\left(f_x\mathrm{g}_y + 2f_y\mathrm{g}_x\right) + 4(1 \\ &+ v) f_{xy}\mathrm{g}_{xy}] \end{aligned} \tag{24}$$

By substituting Eq. (24) into Eq. (3), the strain energy for a finite volume of a radius Rc around a notch tip is:

$$\begin{aligned} E^{(e)} = \int_0^{R_c}\int_{-\alpha}^{+\alpha} W^{(e)} r dr d\theta \\ = \frac{1}{2E}\{&A_1^2 \frac{R_c^{2\lambda^I}}{2\lambda^I}\int_{-\alpha}^{+\alpha}\left(f_x^2 + f_y^2 - 2v f_x f_y + 2(1+v) f_{xy}^2\right)d\theta \\ &+ A_2^2 \frac{R_c^{2\lambda^{II}}}{2\lambda^{II}}\int_{-\alpha}^{+\alpha}\left(\mathrm{g}_x^2 + \mathrm{g}_y^2 - 2v\mathrm{g}_x\mathrm{g}_y + 2(1+v)\mathrm{g}_{xy}^2\right)d\theta \\ &+ A_1 A_2 \frac{R_c^{(\lambda^I+\lambda^{II})}}{\lambda^I + \lambda^{II}}\int_{-\alpha}^{+\alpha}\left(2f_x\mathrm{g}_x + 2f_y\mathrm{g}_y - 2v\left(f_x\mathrm{g}_y + 2f_y\mathrm{g}_x\right)\right. \\ &\left. + 4(1+v) f_{xy}\mathrm{g}_{xy}\right)d\theta\} \end{aligned} \tag{25}$$

Substituting Eqs. (19) and (20) into Eq. (25) gives a quadratic equation with two unknowns:

$$E^{(e)} = MK_I^2 + NK_{II}^2 + QK_IK_{II} \tag{26}$$

Eq. (26) describes a direct relation between the SIFs and the strain energy of a finite volume around the notch tip. Obviously for pure mode I or mode II, Eq. (26) is capable to compute mode I SIF, K_I ($E^{(e)} = MK_I^2$ for pure mode I) or mode II SIF, K_{II} ($E^{(e)} = NK_{II}^2$ for pure mode II). However, for the mixed mode problems, it is difficult to solve Eq. (26) because of the two unknowns of $K_I \; and \; K_{II}$. In order to compute the mixed mode I/II SIFs from the strain energies in the SEA approach, a control volume is drawn around the crack/notch tip in the singular region. The centre line of the crack/notch divides the control volume into an upper region and a lower region. The integral in the numerical model is simply divided into two. Thus, two integral equations are obtained: one for the region below the bisector (-α to 0), and the other for the region above the bisector (0 to α) as shown in Fig. 3(b). That is,

$$E_1^{(e)} = \int_0^{R_c} \int_{-\alpha}^{0} W^{(e)} r dr d\theta = M_1K_I^2 + N_1K_{II}^2 + Q_1K_IK_{II} \tag{27}$$

$$E_2^{(e)} = \int_0^{R_c} \int_{0}^{+\alpha} W^{(e)} r dr d\theta = M_2K_I^2 + N_2K_{II}^2 + Q_2K_IK_{II} \tag{28}$$

Because of the symmetry, it is obvious that $M_1 = M_2, N_1 = N_2 \; and \; Q_1 = -Q_2$.

According to the above equations, the mode I and II SIFs can be determined:

$$2M_1K_I^2 + 2N_1K_{II}^2 = E_1^{(e)} + E_2^{(e)} \tag{29}$$

$$2Q_1K_IK_{II} = E_1^{(e)} - E_2^{(e)} \tag{30}$$

$$2M_1K_I^4 - \left(E_1^{(e)} + E_2^{(e)}\right)K_I^2 + \frac{N_1\left(E_1^{(e)} - E_2^{(e)}\right)^2}{2Q_1^2} = 0 \tag{31}$$

By solving Eqs. (30) and (31), obviously four solutions are obtained. But usually it is easy to determine the correct answers. Among the four solutions, two solutions have negative values and are, therefore, ignored. The other two solutions have positive values; the smaller one of these two positive values is the correct solution. For few problems, the right values can be determined by using the ratio of the relative displacements of the crack/notch faces [13]. For mixed-mode notched problems, both mode I and mode II SIF values are normalized to give:

$$\kappa_I = \frac{K_I}{\sigma\sqrt{\pi}a^{1-\lambda_I}} \tag{32}$$

$$\kappa_{II} = \frac{K_{II}}{\sigma\sqrt{\pi}a^{1-\lambda_{II}}} \tag{33}$$

4. Results and discussion

4.1 Numerical verification with published results

For the case of a single parallel edge-cracked plate subjected to pure tensile loading, i.e. β = zero, the analytical stress intensity factor K_I is related to the applied stress, the crack length and a correction factor, as expressed by Tada et al. [32]:

$$K_I = Y_I \sigma \sqrt{\pi a} \tag{34}$$

where Y_I is the non-dimensional geometric correction factor and it is usually a function of crack length, a, and plate width, W. As defined by Gross and Brown [33, 34], the geometric correction factor, Y_I, is used for the single parallel edge-cracked plate under mode I opening loading when $a/W \leq 0.6$ [32] and it can be written as:

$$Y_I = 1.122 - 0.231 * \frac{a}{W} + 10.550 * \left(\frac{a}{W}\right)^2 - 21.710 * \left(\frac{a}{W}\right)^3 + 30.382 * \left(\frac{a}{W}\right)^4 \tag{35}$$

The above analytical solution is only available for the single parallel edge-cracked plate with pinned boundary conditions (BC). In terms of the case of *h/H=0.5* and different crack length, *a/W*, under pinned BC and clamped BC, the present work is compared with the published results of Tada et al. [32], Hammond & Fawaz [35], Dao & Mettu [36] and John & Rigling [37], as shown in the Table 1. Fig. 4(a) shows an excellent agreement between the present work and published work. For the single edge-notched plate with pinned boundary conditions, a case of *h/H=0.5*, γ=30º, β = zero and different notch length, *a/W*, was investigated and compared with the results by Chen [38]. A good agreement was indicated in Fig. 4(b). Table 2 shows the comparison of mode I SIF K_I for the case of single edge-notched plate (*h/H=0.5*, *a/W*=0.4, β = zero) between the present work and other published results [39-41]. The percentage differences among these results are less than 1%, which indicates that the results of the present work are in an excellent agreement with the published results. Therefore, the present models were adopted for the following analysis.

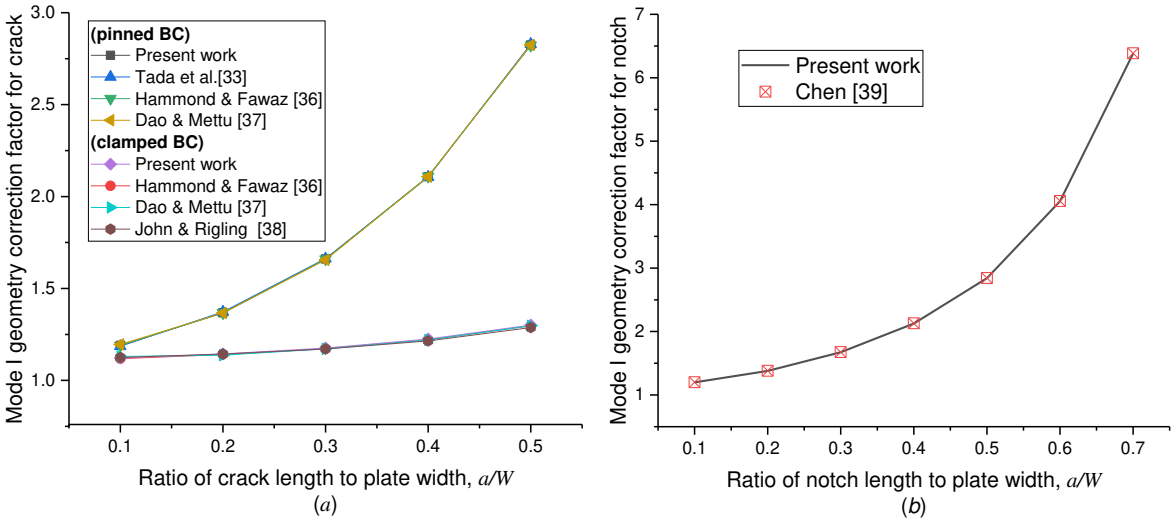

Fig. 4. Comparison of geometry correction factors: (a) single parallel edge-cracked plate under pinned BC and clamped BC; (b) single edge-notched plate under pinned BC.

Table 1
Comparison of mode I SIF K_I for the case of single parallel edge-cracked plate ($h/H=0.5$, β = zero) between present work and other published results.

a/W	Present work		Tada [32]		Hammond & Fawaz [35]		Dao & Mettu [36]		John & Rigling [37]
	pinned	clamped	pinned	clamped	pinned	clamped	pinned	clamped	clamped
0.1	1.1906	1.1183	1.1857	-	1.1890	1.1216	1.1954	1.1302	1.1252
0.2	1.3676	1.1412	1.3727	-	1.3670	1.1443	1.3663	1.1370	1.1435
0.3	1.6604	1.1729	1.6621	-	1.6591	1.1759	1.6553	1.1717	1.1706
0.4	2.1081	1.221	2.1059	-	2.1102	1.2249	2.1079	1.2201	1.2147
0.5	2.8241	1.2966	2.8291	-	2.8226	1.3006	2.8245	1.2966	1.2876

Table 2
Comparison of mode I SIF K_I for the case of single edge-notched plate ($h/H=0.5$, a/W=0.4, β = zero) between present work and other published results.

Method	K_I		Δ (%)	
	$\gamma = 0^o$	$\gamma = 30^o$	$\gamma = 0^o$	$\gamma = 30^o$
BCM [39]	2.113	2.128	0.237	0.047
BEM [40]	2.113	2.129	0.237	0.094
FFEM [41]	2.108	2.125	0.000	-0.094
Present	2.108	2.127	-	-

(Noted that Δ refers to the percentage differences between the present works and published results)

4.2 single edge-cracked plate under tension with pinned and clamped BC

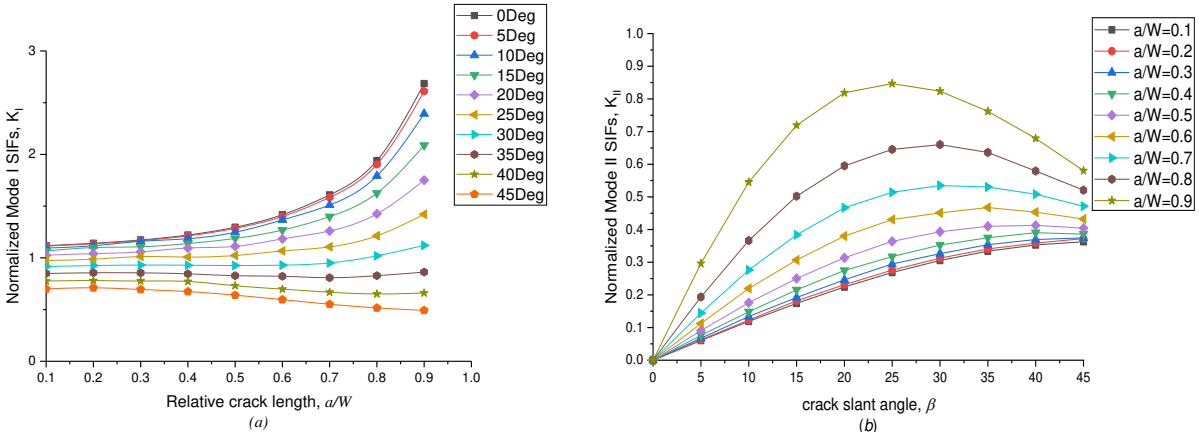

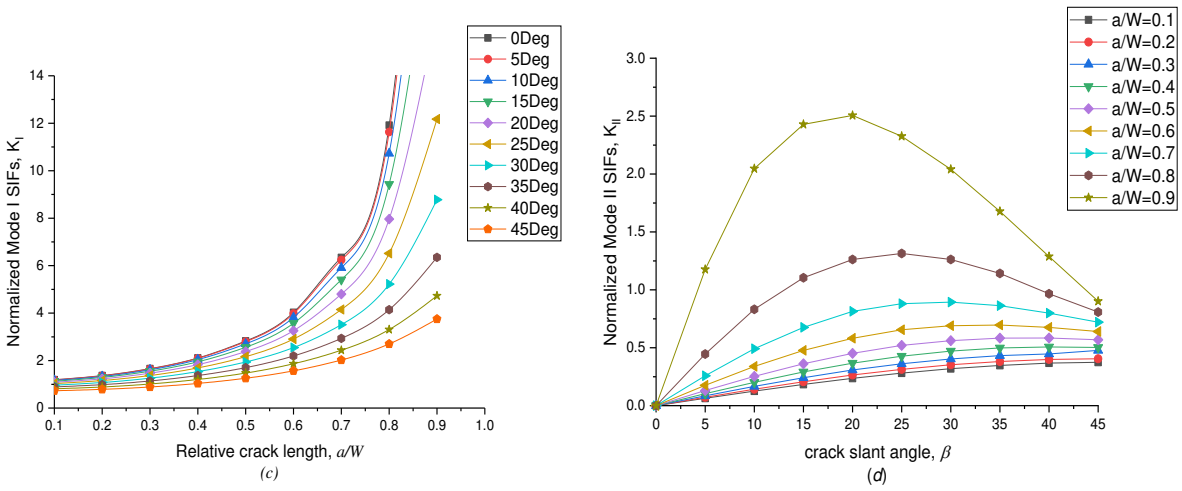

Fig. 5. Variation of stress intensity factors of a single edge-cracked plate with crack angle (β) varying from 0º to 45º and crack length to plate width ratios (a/W) increasing from 0.1 to 0.9, (a) mode I SIF, $K_I/\sigma\sqrt{\pi a}$ under clamped BC; (b) mode II SIF, $K_{II}/\sigma\sqrt{\pi a}$ under clamped BC; (c) mode I SIF, $K_I/\sigma\sqrt{\pi a}$ under pinned BC; (b) mode II SIF, $K_{II}/\sigma\sqrt{\pi a}$ under pinned BC.

Fig. 5 depicts the mixed mode I/II SIFs for various crack positions, angles and lengths under two different boundary conditions of pinned BC and clamped BC. In general, as the ratio of crack length to plate width (a/W) increases from 0.1 to 0.9, mode I SIF increases for the plate under pinned BC. It is noticed that as the crack slanted angle (β) increases from 0º to 45º, mode I SIF decreases and especially when a/W = 0.9, mode I SIF shows a dramatic decline as the crack slanted angle (β) increases to 45º. However, for the plate under clamped BC, as a/W increases from 0.1 to 0.9, mode I SIF increases for $0º \leq \beta \leq 30º$ while it decreases slightly for $35º \leq \beta \leq 45º$. Compared with the pinned BC, to a large extent, the clamped BC diminishes the mode I stress intensity around the crack tip. On the other hand, as the crack slanted angle (β) increases from 0º, there is an obvious shear deformation on the plate and therefore creating mode II SIFs. As β increases from 0º to 45 º, for the plate under either pinned BC or clamped BC, mode II SIF increases. for $0.1 \leq a/W \leq 0.5$. However, for $0.6 \leq a/W \leq 0.9$, mode II SIF initially increases to a maximum value from which it subsequently decreases as β increases from 0º to 45 º. In general, mode II SIFs of the single edge-cracked plate with the clamped BC are smaller than those with the pinned BC. This indicates that the clamped BC effectively reduces the stress intensity around the crack tip.

4.3 single edge-notched plate under tension with pinned and clamped BC

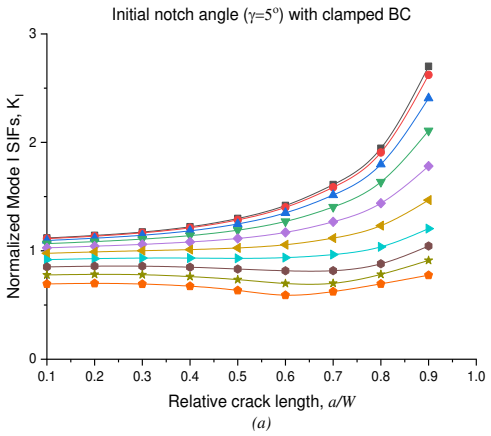

(a)

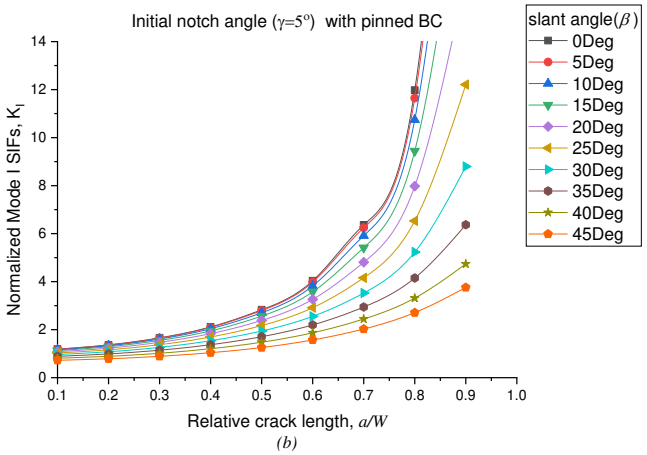

(b)

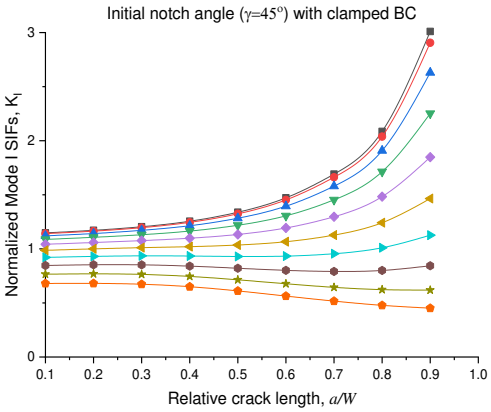

(c)

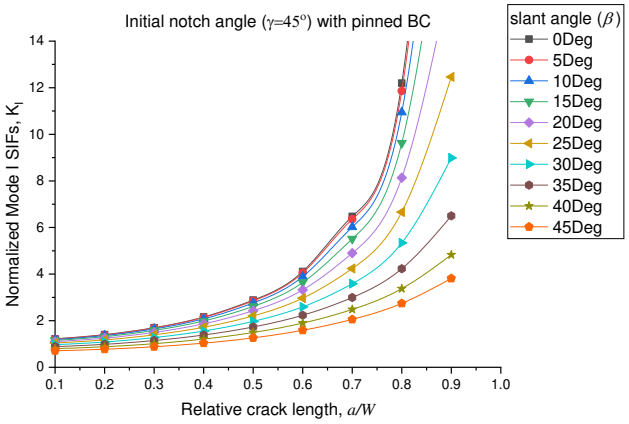

(d)

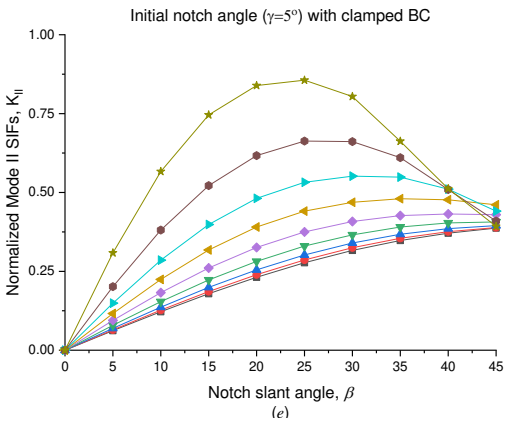

(e)

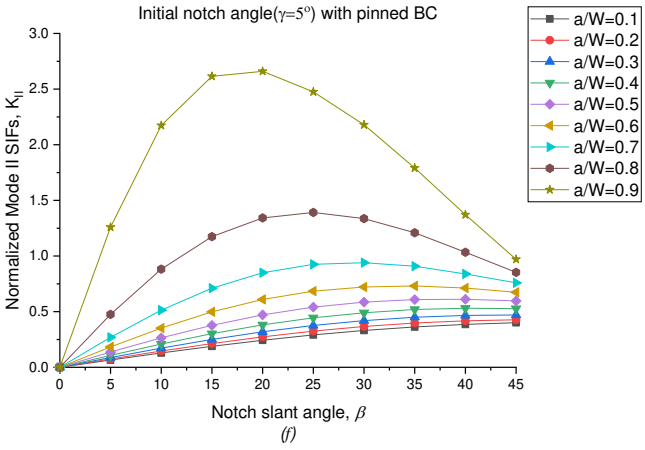

(f)

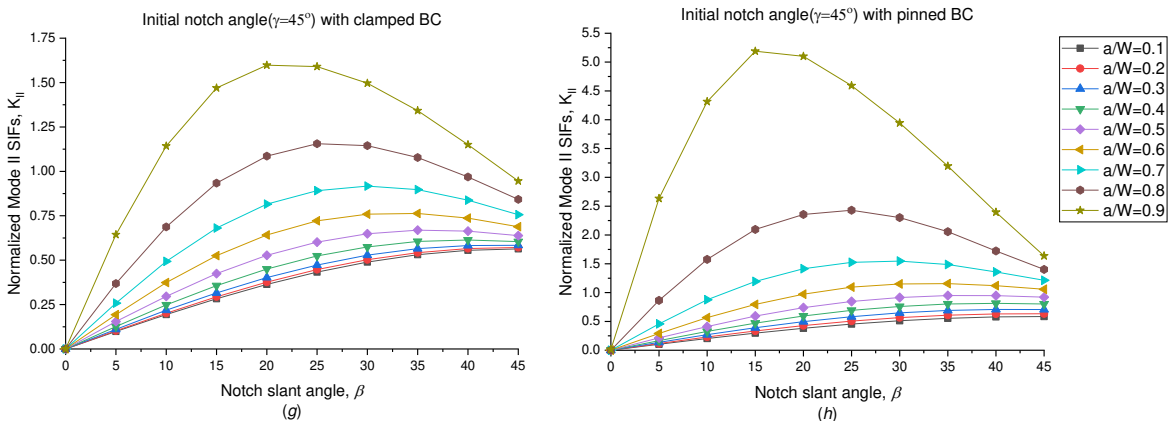

Fig. 6. Variation of stress intensity factors of a single edge-notched plate with slant angle (β) varying from 0º to 45º and notch length to plate width ratios (a/W) increasing from 0.1 to 0.9.

Fig. 6 demonstrates the effect of a/W, β, γ and BCs on mode I and mode II SIFs. In the present work, the notch initial angle (γ) increases from 5º to 45º with an increment of 5º but the finite element analysis results show similar trends in variations of mode I and II SIFs with respect to the crack slant angle for these models. So in this section, the mode I and II SIFs of 5º and 45º notch-initial-angle models are plotted. Similar to the cracked plate, generally as a/W increases from 0.1 to 0.9, mode I SIF increases dramatically in the plate under pinned BC. That increase depends on the notch length and notch slant angle. On the other hand, for the 5º notch-initial-angle plate with clamped BC, as a/W increases, mode I SIF increases continuously when $0º \leqslant \beta \leqslant 30º$ while it shows a slight decline initially and then increase for $35º \leqslant \beta \leqslant 45º$. However, for the plate with 45º initial notch angle with clamped BC, as a/W increases, mode I SIF increases when $0º \leqslant \beta \leqslant 30º$ and decreases slightly for $35º \leqslant \beta \leqslant 45º$. Generally, mode I SIFs of the single edge-notched plate with the clamped BC are smaller than those with the pinned BC. Mode II SIFs show a similar variation between the single edge-notched plate applied with the clamped BC and pinned BC. For instance, when $0.1 \leqslant a/W \leqslant 0.6$, mode II SIFs increase gently as β increases. Besides, for the notched plate under either pinned BC or clamped BC, when a/W=0.8 and 0.9 and β increases from 0º to 45 º, mode II SIF increases initially and decreases greatly while mode I SIF always decreases. It indicates that for a slanted notch, the effect of the mode I stress intensity at the notch tip region is reduced though the mode II shear stress intensity is produced. However, it is found that the mode II SIFs increase as the notch slant angles increase. It is also observed that for notch slant angle range $15º \leqslant \beta \leqslant 25º$, the mode II SIFs attain peak values. This implies that it will be much easier to induce the mode II fracture for this notch slant angle range.

4.4 Effect of pinned and clamped BC on mode I and mode II SIFs

To clarify the effect of initial notch angle, notch length and pinned/clamped BCs on Mode I /II SIFs, Figs. 7 and 8 compare two cases for which $\beta = 20^{\circ}$, $\beta = 45^{\circ}$, a/W changes from 0.6 to 0.9 and γ varies from 0º to 45º under two different boundary conditions. In the figure legend, C denotes clamped BCs, whose results are shown as red symbols in the sub-figures, while P denotes pinned BCs, whose results are shown as black symbols in the sub-figures.

Fig.7 shows the variations of mode I/II SIFs when $a/W = 0.1$ to 0.5 and $\beta = 20^{\circ}$ and 45º. For the case of $\beta = 20^{\circ}$, as γ increases from 0º to 25º, mode I SIF is constant for the plate under either pinned BC or clamped BC, but slightly increases in value as γ increases from 25º to 45º. On the other hand, as γ increases, there is a significant increase in mode II SIF under clamped and pinned BCs. For the case of $\beta = 45^{\circ}$ and $a/W = 0.1$ to 0.4, as γ increases, mode I SIF increases initially and then decreases slightly for the plate under pinned BC. When $a/W = 0.5$, as γ increases, mode I SIF increases initially, remains at a constant value when γ increases from 5º to 35º, and then increases slightly when γ increases from 35º to 45º, for the plate under pinned BC. However, there is a slight decrease in mode I SIF for the plate under clamped BC. Nevertheless, in all cases, as γ increases, mode II SIF increases for the plate subjected to pinned BC or clamped BC. The figure shows that in all cases, the mode I/II SIF values for the plate under pinned BC are larger than those under clamped BC. As β increases from 20º to 45º, the mode I SIF decreases significantly while mode II SIF increases slightly.

In Fig. 8, it can be noticed that for the case of $\beta = 20^{\circ}$, as γ increases, there is a very slight increase in mode I SIF under either pinned BC or clamped BC. On the other hand, as γ increases, mode II SIF increases significantly for the plate with clamped BC while it increases slightly for the plate under pinned BC. For the case of $\beta = 45^{\circ}$ and $a/W = 0.6$, 0.7, 0.8 and 0.9, as γ increases, mode I SIF increases very slightly while mode II SIF shows a distinct increasing trend for the plate under pinned BC. It is similar to the case of $\beta = 20^{\circ}$. However, for $\beta = 45^{\circ}$ and $a/W = 0.6$ for the plate under clamped BC, as γ increases, mode I SIF decreases slightly. However, when $a/W = 0.7$, 0.8 and 0.9, mode I SIF increases dramatically with increasing initial slant angle to reach a maximum followed by a gentle decrease in mode I SIF. Meanwhile, there is an unmistakeable decline in mode II SIF value initially when γ increases from 0º to 5º and then mode II SIF increases as γ increases from 5º to 45º. It can be seen that for the single slant-edge-notch plate, mode I/II SIFs of the cases of $\beta = 20^{\circ}$ are totally different from those of the case of $\beta = 45^{\circ}$; the applied boundary condition is the second main factor to cause this effect. As the slant angle and initial notch angle increase, the symmetrical pattern of stress intensity distributions are disturbed. The figure also shows a contrasting effect of the BCs on the mode I SIFs when $\beta = 45^{\circ}$. It is seen from Fig 8(c) that as a/W increases from 0.6 to 0.9, the mode I SIF values of the plate with clamped BCs increase significantly, whereas the mode I SIF values of the plate with pinned BCs decrease significantly. On the other hand, as a/W increases from 0.6 to 0.9, the mode II SIF values of the plate with clamped or pinned BCs increase significantly.

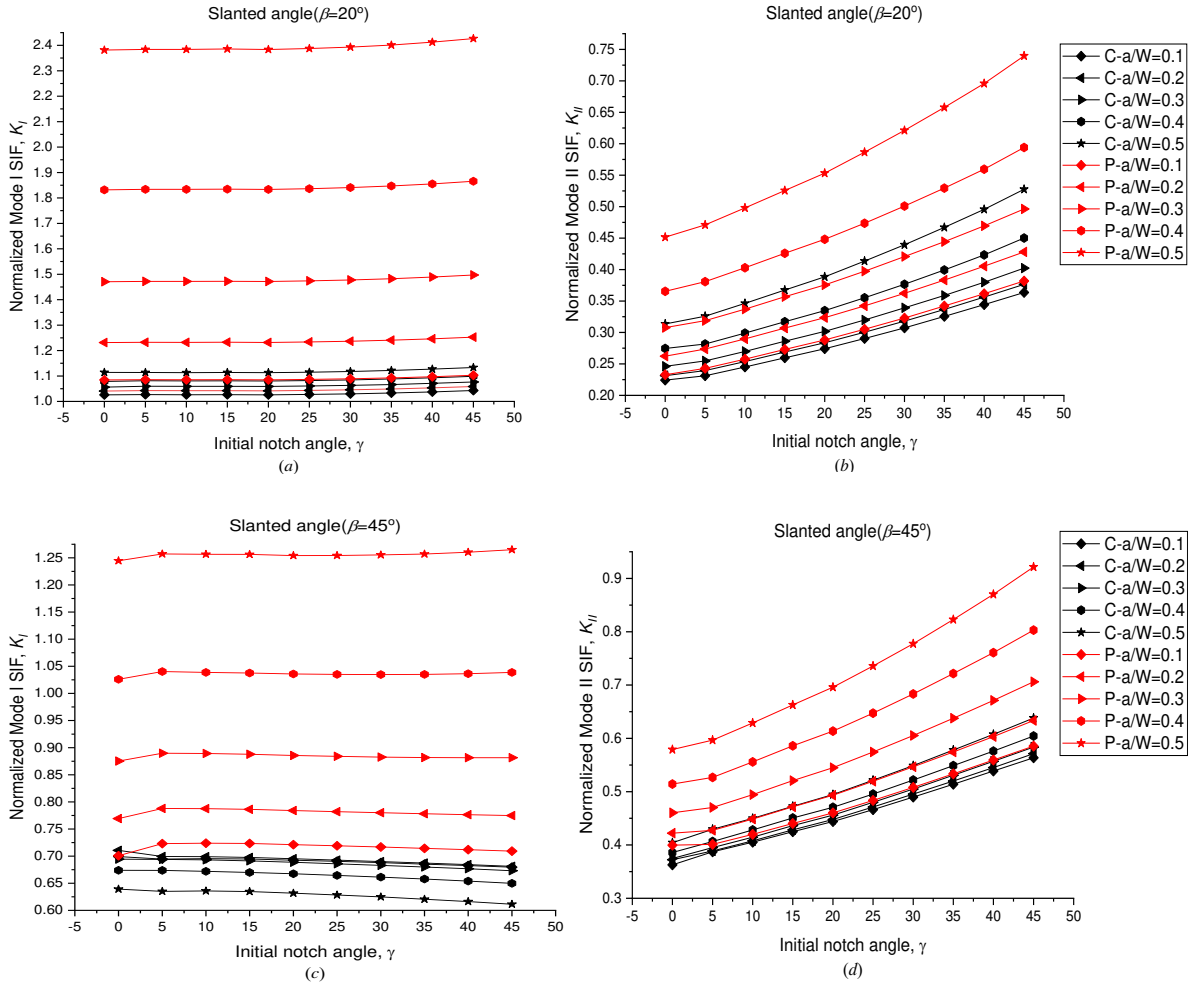

Fig. 7. Effect of initial notch angle, notch length and pinned/clamped BCs on normalized mode I /II SIFs for slant edge crack/notch with slanted angle, (a, b) β = 20º and (c, d) β = 45º, *a/W*=0.1 to 0.5. C denotes clamped BCs (shown as black symbols), P denotes pinned BC (shown as red symbols).

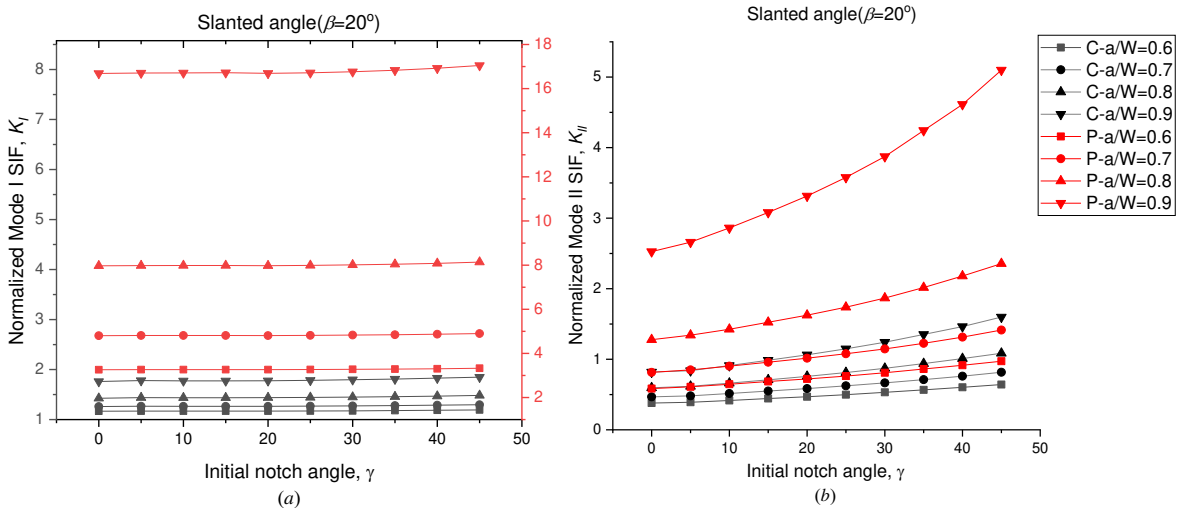

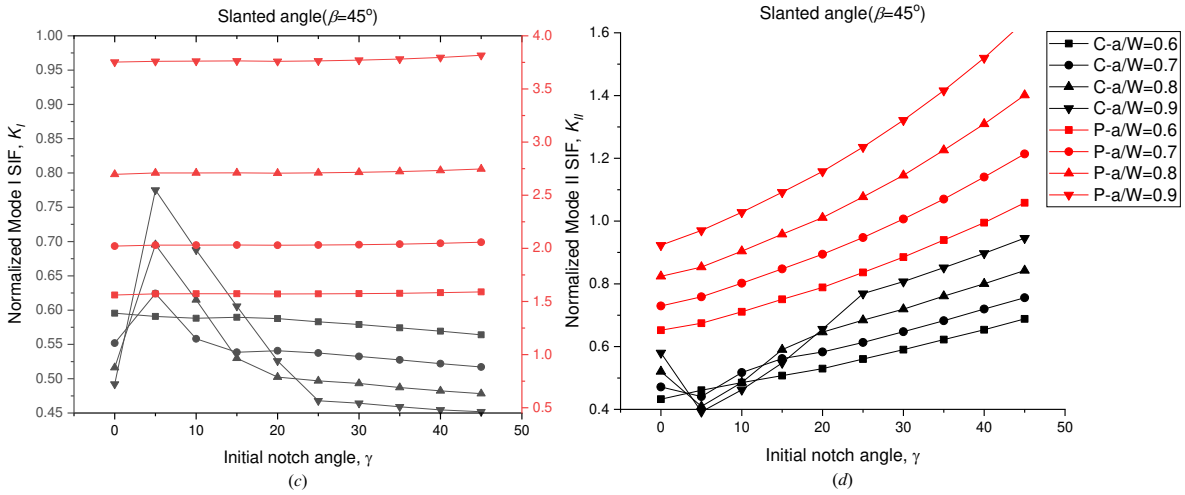

Fig. 8. Effect of initial notch angle, notch length and pinned/clamped BCs on normalized mode I /II SIFs for slant edge crack/notch with slanted angle, (a, b) β = 20º and (c, d) β = 45º, *a/W*=0.6 to 0.9. C denotes clamped BCs (shown as black symbols), P denotes pinned BC (shown as red symbols).

To clarify the sudden change in SIF values between γ = 0º and γ = 5º in the case of the notched plate under clamped BC (when β = 45º) in Fig. 8 (a) and (b), it is necessary to investigate how initial notch angle, γ, in the range 0º to 5º affects the mode I/II SIFs. Fig. 9 shows the variations of mode I/II SIFs when *a/W* = 0.6 to 0.9 and β = 45º and γ = 0º, 0.5º, 1º, 2º, 3º, 4º and 5º. Fig 9(a) shows that as γ changes from 0º to 0.5º, the mode I SIF increases slightly when *a/W* = 0.6, but increases with greater magnitudes as *a/W* increases to 0.7, 0.8 and 0.9 and reaches a peak values when γ = 0.5º and *a/W* = 0.6 to 0.9. As γ changes from 0.5º to 5º, the mode I SIF decreases gradually from the peak values at *a/W* = 0.6 to 0.9. It is seen that the magnitude of the peak values of the mode I SIF at γ = 0.5º is highest when *a/W*=0.9 and lowest when *a/W*=0.6, which indicates that there is a much higher mode I stress intensity at the notch tip region when the notch length increases. On the contrary, Fig 9(b) shows that as γ increases from 0º to 0.5º, the mode II SIF initially decreases slightly when *a/W* = 0.6. However, as *a/W* increases to 0.7, 0.8 and 0.9, the mode II SIF degreases with increasing magnitudes. As γ changes from 0.5º to 5º, the mode II SIF increases gradually. The figure shows that when γ = 0º, the mode II SIF increases as the *a/W* increases from 0.6 to 0.9. However, when γ > 0º the mode II SIF decreases as *a/W* increases from 0.6 to 0.9.

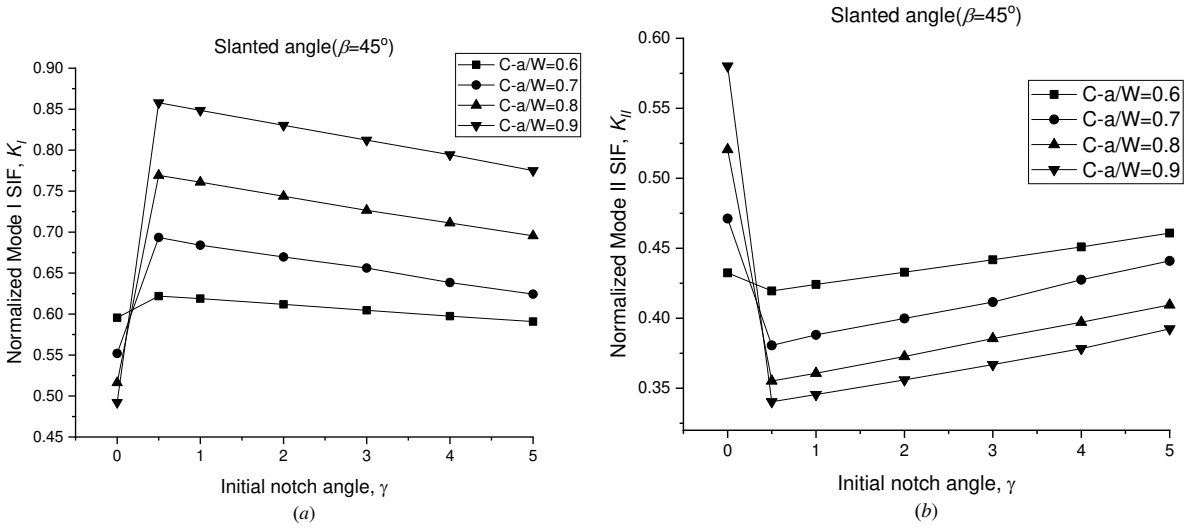

Fig. 9. Zoom in the γ range between 0º and 5º; (a) mode I SIF and (b) mode II SIF for β = 45º, *a/W*=0.6 to 0.9 (C denotes clamped BCs).

5. Conclusions

The present work numerically investigates the mixed mode I/II SIFs for single slant edge-cracked/notched plate under tensile loading. In general, there is a considerable amount of published works on parallel cracked/notched cases. However, there is a lack of published work on mode I/II SIFs for slant cracked/notched cases. This paper provides mode I/II SIF data to fill that gap in the literature. The effects of the crack/notch length to plate width ratio, crack/notch slant angle, notch initial angle and pinned-pinned or clamped-clamped boundary conditions were evaluated. The mode I/II SIFs were obtained using the strain energy approach (SEA) on the computed strain energies of finite element elements around the crack or notch tip. Based on the numerical investigations presented, the following conclusions can be stated:

(1) In general, mode I and II stress intensity factors increase as a function of crack/notch length. Particularly, the magnitude of mode I SIF for the plate under pinned boundary condition is much greater than that under clamped boundary condition.

(2) It can be seen that compared with the single edge-cracked/notched plate under pinned BC, mode I and II SIF values of the plate under clamped BC are much smaller. This is due to the fact that the clamped ends can effectively diminish the crack/notch opening mode and shearing mode stress intensity around the crack/notch tip regions, respectively. It is essential to consider clamped BC on an actual cracked/notched structure for light-weight design.

(3) Under tensile loading, increasing the slant angles decreased magnitude of the mode I SIF for the plate under either pinned or clamped BC. But in most cases, the mode II SIF increases as the slant angle increases for the plate under either pinned or clamped BC.

(4) For the case of slant angle, $\beta = 45°$, when γ increases from 0º to 0.5º, there is a sudden increase in mode I SIF values and a significant decrease in mode II SIF values as a/W approaches 0.9 for the notched plate under clamped BC. This seems to imply that a plate structure of $a/W > 0.5$ with a slant crack of slant angle $\beta = 45°$ is more stable than a plate structure with a slant notch of slant angle $\beta = 45°$ and initial notch angle $\gamma = 0.5°$.

(5) From the engineering point of view, using SIF as a critical parameter to evaluate the cracked/notched plate under pinned-pinned boundary condition represents a conservative approach. However, fracture mechanics design based on the conservative approach for pinned-pinned boundary conditions leads to a relatively heavier design. In the design of aerospace and space structures, where weight is of concern, fracture mechanics design based on clamped-clamped boundary conditions will enable estimation of possible weight savings compared to the traditional conservative design.

6. Reference

1. Erdogan, F. and G. Sih, *On the Crack Extension in Plates Under Plane Loading and Transverse Shear.* Journal of Basic Engineering, 1963. **85**: p. 519-525.DOI: http://dx.doi.org/10.1115/1.3656897.
2. Griffith, A.A., *The Phenomena of Rupture and Flow in Solids.* Philosophical Transactions of the Royal Society of London. Series A, Containing Papers of a Mathematical or Physical Character, 1921. **221**: p. 163-198.DOI: https://doi.org/10.1098/rsta.1921.0006.
3. Sih, G.C., *Some basic problems in fracture mechanics and new concepts.* Engineering Fracture Mechanics, 1973. **5**(2): p. 365-377.DOI: https://doi.org/10.1016/0013-7944(73)90027-1.
4. Sih, G.C., *Strain-energy-density factor applied to mixed mode crack problems.* International Journal of Fracture, 1974. **10**(3): p. 305-321.DOI: https://doi.org/10.1007/BF00035493.
5. Sih, G.C. and B. Macdonald, *Fracture mechanics applied to engineering problems-strain energy density fracture criterion.* Engineering Fracture Mechanics, 1974. **6**(2): p. 361-386.DOI: https://doi.org/10.1016/0013-7944(74)90033-2.
6. Hussain, M., S. Pu, and J. Underwood. *Strain energy release rate for a crack under combined mode I and mode II*. in *Fracture analysis: Proceedings of the 1973 national symposium on fracture mechanics, part II*. 1974. ASTM International.
7. Theocaris, P.S. and N.P. Andrianopoulos, *The mises elastic-plastic boundary as the core region in fracture criteria.* Engineering Fracture Mechanics, 1982. **16**(3): p. 425-432.DOI: https://doi.org/10.1016/0013-7944(82)90120-5.
8. Theocaris, P. and N. Andrianopoulos, *The T-criterion applied to ductile fracture.* International Journal of Fracture, 1982. **20**: p. 125-130.DOI: http://dx.doi.org/10.1007/BF01130617.
9. Theocaris, P.S., G.A. Kardomateas, and N.P. Andrianopoulos, *Experimental study of the T-criterion in ductile fractures.* Engineering Fracture Mechanics, 1983. **17**(5): p. 439-447.DOI: https://doi.org/10.1016/0013-7944(83)90040-1.
10. Kong, X.M., N. Schlüter, and W. Dahl, *Effect of triaxial stress on mixed-mode fracture.* Engineering Fracture Mechanics, 1995. **52**(2): p. 379-388.DOI: https://doi.org/10.1016/0013-7944(94)00228-A.

11. Berto, F. and P. Lazzarin, *Relationships between J-integral and the strain energy evaluated in a finite volume surrounding the tip of sharp and blunt V-notches.* International Journal of Solids and Structures, 2007. **44**(14): p. 4621-4645.DOI: https://doi.org/10.1016/j.ijsolstr.2006.11.041.
12. Lazzarin, P. and F. Berto, *Some Expressions for the Strain Energy in a Finite Volume Surrounding the Root of Blunt V-notches.* International Journal of Fracture, 2005. **135**(1): p. 161-185.DOI: https://doi.org/10.1007/s10704-005-3943-6.
13. Lazzarin, P., F. Berto, and M. Zappalorto, *Rapid calculations of notch stress intensity factors based on averaged strain energy density from coarse meshes: Theoretical bases and applications.* International Journal of Fatigue, 2010. **32**(10): p. 1559-1567.DOI: https://doi.org/10.1016/j.ijfatigue.2010.02.017.
14. Lazzarin, P. and S. Filippi, *A generalized stress intensity factor to be applied to rounded V-shaped notches.* International Journal of Solids and Structures, 2006. **43**(9): p. 2461-2478.DOI: https://doi.org/10.1016/j.ijsolstr.2005.03.007.
15. Lazzarin, P. and R. Zambardi, *A finite-volume-energy based approach to predict the static and fatigue behavior of components with sharp V-shaped notches.* International Journal of Fracture, 2001. **112**(3): p. 275-298.DOI: https://doi.org/10.1023/A:1013595930617.
16. Lazzarin, P. and M. Zappalorto, *Plastic notch stress intensity factors for pointed V-notches under antiplane shear loading.* International Journal of Fracture, 2008. **152**(1): p. 1-25.DOI: https://doi.org/10.1007/s10704-008-9260-0.
17. Radaj, D., F. Berto, and P. Lazzarin, *Local fatigue strength parameters for welded joints based on strain energy density with inclusion of small-size notches.* Engineering Fracture Mechanics, 2009. **76**(8): p. 1109-1130.DOI: https://doi.org/10.1016/j.engfracmech.2009.01.009.
18. Zappalorto, M. and P. Lazzarin, *Strain energy-based evaluations of plastic notch stress intensity factors at pointed V-notches under tension.* Engineering Fracture Mechanics, 2011. **78**(15): p. 2691-2706.DOI: https://doi.org/10.1016/j.engfracmech.2011.07.005.
19. Treifi, M. and S.O. Oyadiji, *Strain energy approach to compute stress intensity factors for isotropic homogeneous and bi-material V-notches.* International Journal of Solids and Structures, 2013. **50**(14): p. 2196-2212.DOI: https://doi.org/10.1016/j.ijsolstr.2013.03.011.
20. Hammouda, M.M.I., A.S. Fayed, and H.E.M. Sallam, *Mode II stress intensity factors for central slant cracks with frictional surfaces in uniaxially compressed plates.* International Journal of Fatigue, 2002. **24**(12): p. 1213-1222.DOI: https://doi.org/10.1016/S0142-1123(02)00048-8.
21. Hammouda, M.M.I., A.S. Fayed, and H.E.M. Sallam, *Stress intensity factors of a central slant crack with frictional surfaces in plates with biaxial loading.* International Journal of Fracture, 2004. **129**(2): p. 141-148.DOI: https://doi.org/10.1023/B:FRAC.0000045714.80342.a3.
22. Hammouda, M.M.I., R.A. Pasha, and A.S. Fayed, *Modelling of cracking sites/development in axial dovetail joints of aero-engine compressor discs.* International Journal of Fatigue, 2007. **29**(1): p. 30-48.DOI: https://doi.org/10.1016/j.ijfatigue.2006.02.049.
23. Henshell, R.D. and K.G. Shaw, *Crack tip finite elements are unnecessary.* International Journal for Numerical Methods in Engineering, 1975. **9**(3): p. 495-507.DOI: https://doi.org/10.1002/nme.1620090302.
24. Barsoum, R.S., *Triangular Quarter-Point Elements as Elastic and Perfectly-Plastic Crack Tip Elements.* International Journal for Numerical Methods in Engineering, 1977. **11**(1): p. 85-98.DOI: https://doi.org/10.1002/nme.1620110109.
25. Barsoum, R.S., *On the use of isoparametric finite elements in linear fracture mechanics.* 1976. **10**(1): p. 25-37.DOI: https://doi.org/10.1002/nme.1620100103.
26. Petit, C., A. Vergne, and X. Zhang, *A comparative numerical review of cracked materials.* Engineering Fracture Mechanics, 1996. **54**(3): p. 423-439.DOI: https://doi.org/10.1016/0013-7944(95)00145-X.
27. Hedayati, E. and M. Vahedi, *Using extended finite element method for computation of the stress intensity factor, crack growth simulation and predicting fatigue crack growth in a slant-cracked plate of 6061-T651 aluminum.* World Journal of Mechanics, 2014. **2014**.DOI: https://doi.org/10.4236/wjm.2014.41003.
28. Version, A., *6.13 Documentation (Abaqus), 2013.* Abaqus user's guide.
29. Bower, A.F., *Applied mechanics of solids*. 2009: CRC press.

30. Williams, M.L., *Stress Singularities Resulting from Various Boundary Conditions in Angular Corners of Plates in Extension.* Journal of Applied Mechanics-Transactions of the Asme, 1952. **19**(4): p. 526-528.DOI: http://dx.doi.org/10.1115/1.4010553.
31. Portela, A., M.H. Aliabadi, and D.P. Rooke, *Efficient boundary element analysis of sharp notched plates.* 1991. **32**(3): p. 445-470.DOI: http://dx.doi.org/10.1002/nme.1620320302.
32. Ewalds, H.L., *Fracture mechanics*, ed. R.J.H. Wanhill. 1984, London: Edward Arnold.
33. William F. Brown, J.E.S., *Plane Strain Crack Toughness Testing of High Strength Metallic Materials*. 1966, West Conshohocken, PA: ASTM International. 129-1966.
34. Gross, B., *Stress-intensity factors for a single-edge-notch tension specimen by boundary collocation of a stress function*. 1964: National Aeronautics and Space Administration.
35. Hammond, M.J. and S.A. Fawaz, *Stress intensity factors of various size single edge-cracked tension specimens: A review and new solutions.* Engineering Fracture Mechanics, 2016. **153**: p. 25-34.DOI: https://doi.org/10.1016/j.engfracmech.2015.12.022.
36. Dao, T. and S. Mettu, *Analysis of an edge cracked specimen subjected to rotationally constrained end displacement.* NASA JSC, 1991. **32171**.
37. John, R. and B. Rigling, *Effect of height to width ratio on K and CMOD solutions for a single edge cracked geometry with clamped ends.* Engineering Fracture Mechanics, 1998. **60**(2): p. 147-156.DOI: https://doi.org/10.1016/S0013-7944(98)00009-5.
38. Chen, D.-H., *Stress intensity factors for V-notched strip under tension or in-plane bending.* International Journal of Fracture, 1994. **70**(1): p. 81-97.DOI: https://doi.org/10.1007/BF00018137.
39. Gross, B. and A. Mendelson, *Plane elastostatic analysis of V-notched plates.* International Journal of Fracture Mechanics, 1972. **8**(3): p. 267-276.DOI: https://doi.org/10.1007/BF00186126.
40. Portela, A., M.H. Aliabadi, and D.P. Rooke, *Efficient boundary element analysis of sharp notched plates.* International Journal for Numerical Methods in Engineering, 1991. **32**(3): p. 445-470.DOI: https://doi.org/10.1002/nme.1620320302.
41. Treifi, M., S.O. Oyadiji, and D.K. Tsang, *Computation of the stress intensity factors of sharp notched plates by the fractal ‐like finite element method.* International Journal for Numerical Methods in Engineering, 2009. **77**(4): p. 558-580.DOI: https://doi.org/10.1002/nme.2425.

Appendix

SIFs values of the single edge-cracked plate (γ=0º) with pinned BC

Crack angle	0		5		10		15		20		25		30		35		40		45	
a/W	K_I	K_{II}	K_I	K_{II}	K_I	K_{II}	K_I	K_{II}	K_I	K_{II}	K_I	K_{II}	K_I	K_{II}	K_I	K_{II}	K_I	K_{II}	K_I	K_{II}
0.1	1.1906	0	1.1830	0.0638	1.1628	0.1256	1.1296	0.1835	1.0844	0.2359	1.0284	0.2813	0.963	0.3189	0.8901	0.3472	0.8109	0.3673	0.7274	0.3743
0.2	1.3676	0	1.3596	0.0721	1.3329	0.1417	1.2896	0.2065	1.2311	0.2645	1.1594	0.3136	1.0767	0.3535	0.9857	0.3815	0.889	0.399	0.789	0.4049
0.3	1.6604	0	1.6491	0.0849	1.6117	0.1661	1.5511	0.2413	1.4702	0.3078	1.3723	0.3616	1.2612	0.4029	1.141	0.4323	1.0157	0.4468	0.8889	0.4772
0.4	2.1081	0	2.0945	0.1032	2.0387	0.2011	1.9493	0.2912	1.8314	0.3665	1.6912	0.4268	1.5356	0.4715	1.3709	0.4984	1.2033	0.5072	1.0376	0.5023
0.5	2.8241	0	2.796	0.1306	2.7063	0.2532	2.5644	0.3613	2.3810	0.4516	2.1683	0.5207	1.9392	0.5608	1.7049	0.5831	1.4745	0.5842	1.2544	0.5688
0.6	4.0294	0	3.9798	0.1758	3.8203	0.3384	3.5724	0.4772	3.2596	0.5812	2.9092	0.6551	2.5469	0.6901	2.1942	0.6965	1.8659	0.6761	1.5689	0.6403
0.7	6.3438	0	6.2411	0.2582	5.9099	0.4911	5.4092	0.6756	4.801	0.814	4.1507	0.8807	3.515	0.8935	2.9363	0.8632	2.4383	0.7987	2.0252	0.7203
0.8	11.917	0	11.632	0.4453	10.726	0.8319	9.4296	1.1043	7.9635	1.262	6.5183	1.3142	5.2213	1.2621	4.143	1.1414	3.3077	0.9663	2.7023	0.8084
0.9	34.409	0	32.750	1.1767	28.057	2.0468	22.162	2.4287	16.667	2.5059	12.173	2.3258	8.7792	2.0408	6.3518	1.6774	4.7286	1.2882	3.751	0.9012

SIFs values of the single edge-cracked plate (γ=0º) with clamped BC

Crack angle	0		5		10		15		20		25		30		35		40		45	
a/W	K_I	K_{II}	K_I	K_{II}	K_I	K_{II}	K_I	K_{II}	K_I	K_{II}	K_I	K_{II}	K_I	K_{II}	K_I	K_{II}	K_I	K_{II}	K_I	K_{II}
0.1	1.1183	0	1.1137	0.0604	1.0945	0.1188	1.0658	0.1741	1.0253	0.2242	0.9748	0.2684	0.9155	0.3054	0.8489	0.3338	0.7762	0.3528	0.6992	0.3627
0.2	1.1412	0	1.1358	0.0625	1.1170	0.1231	1.0993	0.1821	1.0409	0.2313	0.9874	0.2758	0.9251	0.3124	0.8554	0.3406	0.7802	0.3585	0.7106	0.3723
0.3	1.1729	0	1.1665	0.0673	1.1596	0.1338	1.1070	0.1920	1.0579	0.2462	1.0115	0.2944	0.9301	0.3263	0.8552	0.3536	0.7761	0.3695	0.6944	0.3747
0.4	1.221	0	1.2124	0.0761	1.1848	0.1484	1.1385	0.2153	1.0952	0.2747	1.0078	0.3173	0.9289	0.3525	0.8451	0.3751	0.7715	0.3904	0.6739	0.3860
0.5	1.2966	0	1.2853	0.0905	1.2473	0.1759	1.1880	0.2501	1.1109	0.3136	1.0226	0.3639	0.9258	0.3933	0.8277	0.4100	0.7311	0.4129	0.6391	0.4043
0.6	1.417	0	1.4002	0.1124	1.3665	0.2195	1.2680	0.3069	1.1837	0.3800	1.0659	0.4307	0.9292	0.4511	0.8216	0.4674	0.6977	0.4534	0.5955	0.4324
0.7	1.6085	0	1.5846	0.1442	1.5114	0.2765	1.3994	0.3837	1.2594	0.4670	1.1061	0.5141	0.9510	0.5349	0.8078	0.5303	0.6681	0.5083	0.5520	0.4713
0.8	1.9395	0	1.9032	0.1935	1.7923	0.3665	1.6260	0.5022	1.4257	0.5952	1.2133	0.6455	1.0197	0.6601	0.8273	0.6360	0.6510	0.5791	0.5162	0.5206
0.9	2.6854	0	2.6103	0.2962	2.3928	0.5454	2.0884	0.7193	1.7514	0.8188	1.4211	0.8470	1.1206	0.8237	0.8624	0.7621	0.6603	0.6792	0.4922	0.5802

SIFs values of the single edge-notched plate (γ=5º) with pinned BC

Slant angle	0		5		10		15		20		25		30		35		40		45	
a/W	K_I	K_{II}	K_I	K_{II}	K_I	K_{II}	K_I	K_{II}	K_I	K_{II}	K_I	K_{II}	K_I	K_{II}	K_I	K_{II}	K_I	K_{II}	K_I	K_{II}
0.1	1.1881	0	1.1815	0.0653	1.1619	0.1288	1.1296	0.1886	1.0856	0.2430	1.0307	0.2910	0.9662	0.3310	0.8929	0.3627	0.8119	0.3857	0.7230	0.4011
0.2	1.3675	0	1.3588	0.0745	1.3327	0.1464	1.2902	0.2134	1.2326	0.2737	1.1617	0.3253	1.0799	0.3668	0.9889	0.3978	0.8913	0.4174	0.7878	0.4274
0.3	1.6613	0	1.6489	0.0877	1.6120	0.1721	1.5520	0.2504	1.4720	0.3188	1.3750	0.3757	1.2647	0.4195	1.1448	0.4497	1.0192	0.4659	0.8898	0.4704
0.4	2.1137	0	2.0949	0.1071	2.0397	0.2091	1.9508	0.3021	1.8340	0.3808	1.6943	0.4448	1.5398	0.4900	1.3750	0.5192	1.2070	0.5309	1.0403	0.5268
0.5	2.8274	0	2.7968	0.1373	2.7076	0.2645	2.5669	0.3772	2.3842	0.4710	2.1723	0.5406	1.9438	0.5860	1.7092	0.6090	1.4791	0.6108	1.2572	0.5966
0.6	4.0372	0	3.9827	0.1831	3.8236	0.3524	3.5761	0.4984	3.2642	0.6098	2.9150	0.6845	2.5535	0.7219	2.1993	0.7305	1.8697	0.7118	1.5720	0.6744
0.7	6.3626	0	6.2473	0.2691	5.9164	0.5136	5.4169	0.7108	4.8094	0.8501	4.1597	0.9257	3.5246	0.9400	2.9436	0.9087	2.4458	0.8388	2.0301	0.7587
0.8	11.975	0	11.647	0.4751	10.742	0.8819	9.4452	1.1736	7.9787	1.3418	6.5310	1.3917	5.2342	1.3363	4.1528	1.2089	3.3168	1.0338	2.7090	0.8535
0.9	34.693	0	32.820	1.2589	28.068	2.1728	22.213	2.6145	16.708	2.6596	12.208	2.4757	8.7998	2.1789	6.3685	1.7909	4.7395	1.3708	3.7600	0.9702

SIFs values of the single edge-notched plate (γ=5º) with clamped BC

Slant angle	0		5		10		15		20		25		30		35		40		45	
a/W	K_I	K_{II}	K_I	K_{II}	K_I	K_{II}	K_I	K_{II}	K_I	K_{II}	K_I	K_{II}	K_I	K_{II}	K_I	K_{II}	K_I	K_{II}	K_I	K_{II}
0.1	1.1184	0	1.1125	0.0619	1.0950	0.1221	1.0662	0.1790	1.0268	0.2311	0.9772	0.2774	0.9187	0.3163	0.8518	0.3476	0.7773	0.3709	0.6945	0.3871
0.2	1.1414	0	1.1351	0.0646	1.1161	0.1271	1.0850	0.1859	1.0425	0.2395	0.9898	0.2861	0.9281	0.3248	0.8584	0.3550	0.7823	0.3757	0.6994	0.3887
0.3	1.1733	0	1.1659	0.0694	1.1439	0.1365	1.1079	0.1992	1.0597	0.2547	1.0009	0.3019	0.9333	0.3397	0.8586	0.3677	0.7789	0.3855	0.6939	0.3951
0.4	1.2215	0	1.2121	0.0788	1.1844	0.1540	1.1398	0.2228	1.0812	0.2816	1.0108	0.3302	0.9329	0.3657	0.8487	0.3905	0.7619	0.4036	0.6737	0.4065
0.5	1.2977	0	1.2849	0.0945	1.2480	0.1826	1.1897	0.2607	1.1139	0.3258	1.0260	0.3749	0.9308	0.4081	0.8320	0.4268	0.7342	0.4319	0.6350	0.4295
0.6	1.4179	0	1.4006	0.1164	1.3498	0.2244	1.2705	0.3177	1.1699	0.3904	1.0563	0.4407	0.9373	0.4688	0.8161	0.4803	0.6986	0.4767	0.5908	0.4608
0.7	1.6105	0	1.5858	0.1491	1.5141	0.2856	1.4043	0.3984	1.2676	0.4814	1.1171	0.5321	0.9650	0.5518	0.8168	0.5487	0.7003	0.5105	0.6243	0.4410
0.8	1.9449	0	1.9065	0.2015	1.7979	0.3810	1.6352	0.5218	1.4390	0.6168	1.2318	0.6631	1.0368	0.6614	0.8803	0.6103	0.7830	0.5093	0.6955	0.4095

0.9	2.7016	0	2.6222	0.3084	2.4072	0.5665	2.1077	0.7460	1.7806	0.8389	1.4679	0.8560	1.2042	0.8042	1.0443	0.6625	0.9116	0.5118	0.7750	0.3924

SIFs values of the single edge-notched plate (γ=10º) with pinned BC

Slant angle	0		5		10		15		20		25		30		35		40		45	
a/W	K_I	K_{II}	K_I	K_{II}	K_I	K_{II}	K_I	K_{II}	K_I	K_{II}	K_I	K_{II}	K_I	K_{II}	K_I	K_{II}	K_I	K_{II}	K_I	K_{II}
0.1	1.1889	0	1.1822	0.0693	1.1624	0.1366	1.1297	0.2000	1.0852	0.2576	1.0298	0.3082	0.9648	0.3502	0.8912	0.3831	0.8108	0.4060	0.7238	0.4199
0.2	1.3684	0	1.3596	0.0790	1.3333	0.1550	1.2903	0.2263	1.2323	0.2898	1.1608	0.3446	1.0785	0.3881	0.9873	0.4201	0.8896	0.4402	0.7875	0.4487
0.3	1.6622	0	1.6497	0.0932	1.6126	0.1824	1.5523	0.2650	1.4718	0.3370	1.3742	0.3975	1.2634	0.4437	1.1434	0.4747	1.0171	0.4921	0.8892	0.4944
0.4	2.1145	0	2.0957	0.1134	2.0403	0.2208	1.9512	0.3190	1.8338	0.4028	1.6937	0.4706	1.5389	0.5172	1.3737	0.5485	1.2057	0.5602	1.0387	0.5558
0.5	2.8282	0	2.7976	0.1442	2.7082	0.2800	2.5675	0.3976	2.3842	0.4980	2.1719	0.5719	1.9429	0.6195	1.7085	0.6432	1.4786	0.6438	1.2566	0.6288
0.6	4.0377	0	3.9834	0.1932	3.8241	0.3740	3.5767	0.5271	3.2643	0.6457	2.9150	0.7242	2.5534	0.7630	2.1992	0.7719	1.8702	0.7505	1.5723	0.7111
0.7	6.3629	0	6.2477	0.2861	5.9170	0.5451	5.4172	0.7557	4.8102	0.9021	4.1606	0.9817	3.5251	0.9956	2.9447	0.9614	2.4462	0.8868	2.0302	0.8021
0.8	11.975	0	11.647	0.5082	10.744	0.9378	9.4468	1.2488	7.9813	1.4255	6.5332	1.4816	5.2360	1.4207	4.1558	1.2815	3.3183	1.0964	2.7093	0.9041
0.9	34.687	0	32.819	1.3750	28.071	2.3385	22.213	2.8284	16.711	2.8616	12.209	2.6613	8.8054	2.3252	6.3737	1.9080	4.7423	1.4604	3.7618	1.0281

SIFs values of the single edge-notched plate (γ=10º) with clamped BC

Slant angle	0		5		10		15		20		25		30		35		40		45	
a/W	K_I	K_{II}	K_I	K_{II}	K_I	K_{II}	K_I	K_{II}	K_I	K_{II}	K_I	K_{II}	K_I	K_{II}	K_I	K_{II}	K_I	K_{II}	K_I	K_{II}
0.1	1.1192	0	1.1132	0.0657	1.0955	0.1295	1.0663	0.1899	1.0263	0.2451	0.9763	0.2938	0.9173	0.3347	0.8501	0.3672	0.7761	0.3904	0.6953	0.4052
0.2	1.1421	0	1.1357	0.0685	1.1165	0.1347	1.0850	0.1972	1.0421	0.2537	0.9888	0.3032	0.9266	0.3437	0.8567	0.3749	0.7805	0.3962	0.6990	0.4078
0.3	1.1741	0	1.1665	0.0739	1.1443	0.1449	1.1080	0.2112	1.0593	0.2698	0.9998	0.3200	0.9317	0.3597	0.8569	0.3884	0.7765	0.4072	0.6932	0.4147
0.4	1.2224	0	1.2129	0.0838	1.1850	0.1634	1.1399	0.2362	1.0806	0.2989	1.0096	0.3503	0.9312	0.3871	0.8465	0.4132	0.7598	0.4260	0.6719	0.4281
0.5	1.2989	0	1.2861	0.1000	1.2487	0.1943	1.1900	0.2765	1.1132	0.3463	1.0244	0.3985	0.9283	0.4332	0.8293	0.4521	0.7321	0.4556	0.6359	0.4499
0.6	1.4198	0	1.4023	0.1238	1.3509	0.2395	1.2707	0.3383	1.1687	0.4159	1.0538	0.4694	0.9335	0.4987	0.8121	0.5101	0.6975	0.5024	0.5881	0.4854
0.7	1.6141	0	1.5890	0.1594	1.5162	0.3051	1.4045	0.4261	1.2658	0.5145	1.1128	0.5689	0.9577	0.5903	0.8071	0.5875	0.6741	0.5586	0.5582	0.5175
0.8	1.9526	0	1.9133	0.2165	1.8029	0.4084	1.6369	0.5594	1.4371	0.6606	1.2237	0.7131	1.0185	0.7167	0.8357	0.6808	0.6956	0.6051	0.6150	0.4856
0.9	2.7220	0	2.6403	0.3365	2.4197	0.6146	2.1110	0.8104	1.7740	0.9108	1.4454	0.9358	1.1547	0.8951	0.9455	0.7765	0.8108	0.6077	0.6877	0.4622

SIFs values of the single edge-notched plate (γ=20º) with pinned BC

Slant angle	0		5		10		15		20		25		30		35		40		45	
a/W	K_I	K_{II}	K_I	K_{II}	K_I	K_{II}	K_I	K_{II}	K_I	K_{II}	K_I	K_{II}	K_I	K_{II}	K_I	K_{II}	K_I	K_{II}	K_I	K_{II}
0.1	1.1907	0	1.1840	0.0777	1.1637	0.1528	1.1301	0.2241	1.0849	0.2881	1.0284	0.3438	0.9622	0.3900	0.8877	0.4253	0.8069	0.4488	0.7211	0.4603
0.2	1.3707	0	1.3612	0.0883	1.3343	0.1732	1.2910	0.2527	1.2319	0.3236	1.1596	0.3839	1.0762	0.4316	0.9840	0.4661	0.8858	0.4871	0.7840	0.4934
0.3	1.6640	0	1.6513	0.1035	1.6138	0.2034	1.5528	0.2951	1.4716	0.3755	1.3731	0.4415	1.2612	0.4932	1.1403	0.5268	1.0137	0.5445	0.8857	0.5449
0.4	2.1160	0	2.0970	0.1266	2.0412	0.2452	1.9516	0.3553	1.8334	0.4481	1.6924	0.5238	1.5366	0.5757	1.3713	0.6088	1.2028	0.6206	1.0359	0.6135
0.5	2.8286	0	2.7979	0.1600	2.7087	0.3116	2.5673	0.4443	2.3837	0.5532	2.1713	0.6369	1.9418	0.6885	1.7067	0.7158	1.4758	0.7151	1.2542	0.6960
0.6	4.0365	0	3.9821	0.2157	3.8229	0.4150	3.5757	0.5900	3.2640	0.7205	2.9143	0.8092	2.5522	0.8505	2.1985	0.8604	1.8694	0.8337	1.5710	0.7885
0.7	6.3586	0	6.2420	0.3210	5.9126	0.6166	5.4143	0.8475	4.8078	1.0152	4.1596	1.1034	3.5250	1.1157	2.9448	1.0723	2.4453	0.9913	2.0289	0.8942
0.8	11.964	0	11.632	0.5844	10.732	1.0694	9.4397	1.4243	7.9751	1.6246	6.5327	1.6766	5.2373	1.6052	4.1553	1.4475	3.3183	1.2294	2.7073	1.0108
0.9	34.572	0	32.720	1.5738	28.010	2.7127	22.173	3.2793	16.691	3.3137	12.200	3.0692	8.8059	2.6581	6.3746	2.1668	4.7427	1.6532	3.7597	1.1582

SIFs values of the single edge-notched plate (γ=20º) with clamped BC

Slant angle	0		5		10		15		20		25		30		35		40		45	
a/W	K_I	K_{II}	K_I	K_{II}	K_I	K_{II}	K_I	K_{II}	K_I	K_{II}	K_I	K_{II}	K_I	K_{II}	K_I	K_{II}	K_I	K_{II}	K_I	K_{II}
0.1	1.1209	0	1.1149	0.0736	1.0967	0.1449	1.0667	0.2128	1.0260	0.2741	0.9749	0.3278	0.9148	0.3728	0.8467	0.4077	0.7722	0.4315	0.6925	0.4440
0.2	1.1444	0	1.1374	0.0768	1.1175	0.1509	1.0856	0.2206	1.0417	0.2837	0.9875	0.3382	0.9242	0.3826	0.8533	0.4161	0.7763	0.4383	0.6952	0.4479
0.3	1.1761	0	1.1684	0.0826	1.1457	0.1624	1.1086	0.2362	1.0590	0.3017	0.9985	0.3565	0.9290	0.4008	0.8531	0.4315	0.7722	0.4504	0.6887	0.4560
0.4	1.2248	0	1.2151	0.0943	1.1866	0.1830	1.1407	0.2651	1.0802	0.3348	1.0079	0.3920	0.9280	0.4326	0.8427	0.4596	0.7553	0.4718	0.6675	0.4707
0.5	1.3022	0	1.2891	0.1124	1.2511	0.2187	1.1910	0.3118	1.1130	0.3885	1.0227	0.4472	0.9252	0.4844	0.8248	0.5050	0.7265	0.5062	0.6317	0.4946
0.6	1.4250	0	1.4071	0.1400	1.3546	0.2696	1.2726	0.3825	1.1690	0.4687	1.0517	0.5288	0.9292	0.5601	0.8071	0.5707	0.6926	0.5577	0.5877	0.5299
0.7	1.6235	0	1.5973	0.1811	1.5227	0.3477	1.4083	0.4832	1.2658	0.5842	1.1096	0.6448	0.9514	0.6670	0.8003	0.6587	0.6629	0.6275	0.5408	0.5831
0.8	1.9724	0	1.9309	0.2499	1.8165	0.4693	1.6449	0.6418	1.4379	0.7576	1.2195	0.8135	1.0073	0.8177	0.8126	0.7836	0.6458	0.7186	0.5024	0.6462

0.9	2.7718	0	2.6849	0.3951	2.4528	0.7225	2.1298	0.9476	1.7766	1.0622	1.4338	1.0882	1.1256	1.0449	0.8659	0.9502	0.6559	0.8295	0.5259	0.6559

SIFs values of the single edge-notched plate (γ=25º) with pinned BC

Slant angle	0		5		10		15		20		25		30		35		40		45	
a/W	K_I	K_{II}	K_I	K_{II}	K_I	K_{II}	K_I	K_{II}	K_I	K_{II}	K_I	K_{II}	K_I	K_{II}	K_I	K_{II}	K_I	K_{II}	K_I	K_{II}
0.1	1.1941	0	1.1869	0.0823	1.1663	0.1619	1.1324	0.2373	1.0865	0.3051	1.0292	0.3641	0.9622	0.4123	0.8870	0.4492	0.8054	0.4726	0.7191	0.4836
0.2	1.3739	0	1.3646	0.0932	1.3375	0.1837	1.2935	0.2675	1.2338	0.3423	1.1607	0.4062	1.0765	0.4560	0.9835	0.4922	0.8846	0.5134	0.7820	0.5194
0.3	1.6678	0	1.6550	0.1093	1.6173	0.2151	1.5559	0.3126	1.4740	0.3974	1.3747	0.4674	1.2620	0.5213	1.1403	0.5561	1.0130	0.5741	0.8840	0.5744
0.4	2.1203	0	2.1008	0.1329	2.0450	0.2607	1.9549	0.3761	1.8363	0.4737	1.6949	0.5534	1.5382	0.6084	1.3720	0.6435	1.2029	0.6545	1.0351	0.6473
0.5	2.8337	0.0002	2.8029	0.1696	2.7132	0.3290	2.5717	0.4692	2.3874	0.5866	2.1743	0.6721	1.9440	0.7285	1.7085	0.7569	1.4766	0.7561	1.2543	0.7357
0.6	4.0428	0.0002	3.9883	0.2312	3.8288	0.4420	3.5814	0.6250	3.2692	0.7618	2.9183	0.8597	2.5558	0.9016	2.2011	0.9107	1.8710	0.8830	1.5716	0.8362
0.7	6.3682	0.0015	6.2513	0.3399	5.9223	0.6542	5.4223	0.9050	4.8167	1.0783	4.1664	1.1728	3.5299	1.1872	2.9482	1.1430	2.4485	1.0508	2.0308	0.9474
0.8	11.979	0.0013	11.648	0.6164	10.748	1.1527	9.4537	1.5264	7.9898	1.7379	6.5438	1.7968	5.2456	1.7189	4.1619	1.5493	3.3222	1.3140	2.7101	1.0771
0.9	34.630	0.0116	32.775	1.6975	28.059	2.9321	22.207	3.5805	16.717	3.5779	12.225	3.2909	8.8214	2.8656	6.3854	2.3324	4.7493	1.7718	3.7639	1.2359

SIFs values of the single edge-notched plate (γ=25º) with clamped BC

Slant angle	0		5		10		15		20		25		30		35		40		45	
a/W	K_I	K_{II}	K_I	K_{II}	K_I	K_{II}	K_I	K_{II}	K_I	K_{II}	K_I	K_{II}	K_I	K_{II}	K_I	K_{II}	K_I	K_{II}	K_I	K_{II}
0.1	1.1241	0	1.1177	0.0780	1.0993	0.1536	1.0688	0.2254	1.0275	0.2903	0.9756	0.3472	0.9147	0.3941	0.8458	0.4306	0.7706	0.4543	0.6905	0.4663
0.2	1.1472	0	1.1403	0.0811	1.1203	0.1601	1.0877	0.2338	1.0432	0.3003	0.9882	0.3581	0.9241	0.4043	0.8523	0.4394	0.7747	0.4619	0.6926	0.4712
0.3	1.1791	0	1.1714	0.0874	1.1484	0.1722	1.1109	0.2508	1.0606	0.3198	0.9992	0.3779	0.9290	0.4239	0.8522	0.4557	0.7705	0.4746	0.6858	0.4800
0.4	1.2283	0	1.2183	0.0996	1.1895	0.1951	1.1430	0.2815	1.0819	0.3551	1.0088	0.4153	0.9279	0.4580	0.8416	0.4862	0.7533	0.4973	0.6645	0.4955
0.5	1.3064	0	1.2931	0.1197	1.2546	0.2322	1.1939	0.3311	1.1148	0.4135	1.0235	0.4739	0.9247	0.5138	0.8235	0.5345	0.7239	0.5350	0.6283	0.5214
0.6	1.4307	0	1.4125	0.1501	1.3592	0.2881	1.2762	0.4073	1.1714	0.4983	1.0523	0.5633	0.9285	0.5953	0.8053	0.6046	0.6894	0.5901	0.5831	0.5604
0.7	1.6320	0	1.6054	0.1931	1.5298	0.3711	1.4133	0.5172	1.2694	0.6229	1.1107	0.6874	0.9500	0.7110	0.7967	0.7023	0.6589	0.6651	0.5374	0.6133
0.8	1.9872	0	1.9452	0.2671	1.8282	0.5058	1.6531	0.6897	1.4429	0.8124	1.2206	0.8720	1.0051	0.8752	0.8077	0.8378	0.6382	0.7679	0.4969	0.6842
0.9	2.8060	0	2.7165	0.4305	2.4777	0.7859	2.1451	1.0325	1.7850	1.1480	1.4365	1.1697	1.1218	1.1240	0.8556	1.0239	0.6378	0.9001	0.4679	0.7689

SIFs values of the single edge-notched plate (γ=30º) with pinned BC

Slant angle	0		5		10		15		20		25		30		35		40		45	
a/W	K_I	K_{II}	K_I	K_{II}	K_I	K_{II}	K_I	K_{II}	K_I	K_{II}	K_I	K_{II}	K_I	K_{II}	K_I	K_{II}	K_I	K_{II}	K_I	K_{II}
0.1	1.1983	0.0001	1.1911	0.0872	1.1702	0.1718	1.1358	0.2516	1.0889	0.3229	1.0308	0.3853	0.9629	0.4358	0.8867	0.4740	0.8041	0.4978	0.7169	0.5081
0.2	1.3787	6.59E-05	1.3692	0.0993	1.3417	0.1942	1.2971	0.2829	1.2368	0.3622	1.1629	0.4296	1.0776	0.4820	0.9836	0.5195	0.8836	0.5407	0.7800	0.5467
0.3	1.6732	4.16E-05	1.6603	0.1157	1.6222	0.2281	1.5602	0.3299	1.4776	0.4207	1.3776	0.4934	1.2640	0.5501	1.1410	0.5876	1.0127	0.6056	0.8826	0.6053
0.4	2.1265	5.11E-05	2.1070	0.1414	2.0507	0.2756	1.9600	0.3978	1.8408	0.5009	1.6986	0.5857	1.5409	0.6424	1.3740	0.6789	1.2032	0.6918	1.0348	0.6834
0.5	2.8414	0.0002	2.8105	0.1779	2.7199	0.3480	2.5781	0.4968	2.3930	0.6212	2.1790	0.7132	1.9484	0.7696	1.7116	0.8001	1.4787	0.7987	1.2555	0.7774
0.6	4.0532	0.001	3.9981	0.2456	3.8380	0.4721	3.5904	0.6620	3.2770	0.8094	2.9258	0.9109	2.5615	0.9560	2.2061	0.9641	1.8739	0.9385	1.5739	0.8853
0.7	6.3829	0.0001	6.2675	0.3660	5.9362	0.7015	5.4361	0.9649	4.8287	1.1468	4.1766	1.2518	3.5389	1.2641	2.9551	1.2167	2.4530	1.1168	2.0341	1.0066
0.8	12.010	0.0001	11.678	0.6728	10.775	1.2451	9.4775	1.6446	8.0113	1.8678	6.5615	1.9305	5.2598	1.8397	4.1720	1.6536	3.3296	1.4024	2.7150	1.1460
0.9	34.735	0.0018	32.852	1.8901	28.120	3.2544	22.273	3.8777	16.764	3.8737	12.257	3.5866	8.8475	3.0877	6.4027	2.5041	4.7604	1.9075	3.7712	1.3215

SIFs values of the single edge-notched plate (γ=30º) with clamped BC

Slant angle	0		5		10		15		20		25		30		35		40		45	
a/W	K_I	K_{II}	K_I	K_{II}	K_I	K_{II}	K_I	K_{II}	K_I	K_{II}	K_I	K_{II}	K_I	K_{II}	K_I	K_{II}	K_I	K_{II}	K_I	K_{II}
0.1	1.1280	0.0001	1.1216	0.0827	1.1029	0.1630	1.0720	0.2390	1.0297	0.3073	0.9771	0.3675	0.9152	0.4166	0.8454	0.4543	0.7692	0.4784	0.6880	0.4898
0.2	1.1513	0.0001	1.1443	0.0865	1.1239	0.1694	1.0908	0.2475	1.0456	0.3179	0.9898	0.3789	0.9247	0.4275	0.8519	0.4638	0.7732	0.4862	0.6900	0.4955
0.3	1.1835	0.0000	1.1756	0.0928	1.1523	0.1829	1.1141	0.2653	1.0631	0.3391	1.0009	0.3995	0.9297	0.4477	0.8516	0.4815	0.7687	0.5004	0.6829	0.5050
0.4	1.2331	0.0000	1.2229	0.1062	1.1936	0.2071	1.1465	0.2989	1.0845	0.3766	1.0105	0.4405	0.9284	0.4844	0.8410	0.5132	0.7511	0.5251	0.6613	0.5217
0.5	1.3121	0.0001	1.2986	0.1266	1.2593	0.2469	1.1978	0.3521	1.1176	0.4394	1.0250	0.5041	0.9253	0.5441	0.8226	0.5653	0.7217	0.5645	0.6248	0.5489

0.6	1.4381	0.0004	1.4195	0.1602	1.3653	0.3083	1.2814	0.4335	1.1747	0.5311	1.0544	0.5987	0.9286	0.6323	0.8040	0.6405	0.6860	0.6257	0.5790	0.5902
0.7	1.6427	0.0000	1.6159	0.2077	1.5386	0.3981	1.4203	0.5530	1.2741	0.6648	1.1128	0.7340	0.9501	0.7571	0.7945	0.7471	0.6552	0.7041	0.5325	0.6475
0.8	2.0060	0.0000	1.9628	0.2896	1.8430	0.5457	1.6640	0.7426	1.4500	0.8720	1.2236	0.9348	1.0049	0.9351	0.8053	0.8917	0.6343	0.8140	0.4932	0.7192
0.9	2.8462	0.0002	2.7533	0.4747	2.5064	0.8642	2.1660	1.1212	1.7965	1.2417	1.4393	1.2667	1.1211	1.2064	0.8509	1.0954	0.6302	0.9623	0.4643	0.8073

SIFs values of the single edge-notched plate (γ=35º) with pinned BC

Slant angle	0		5		10		15		20		25		30		35		40		45	
a/W	K_I	K_{II}	K_I	K_{II}	K_I	K_{II}	K_I	K_{II}	K_I	K_{II}	K_I	K_{II}	K_I	K_{II}	K_I	K_{II}	K_I	K_{II}	K_I	K_{II}
0.1	1.2036	0.0001	1.1965	0.0925	1.1751	0.1822	1.1400	0.2663	1.0925	0.3420	1.0334	0.4073	0.9643	0.4602	0.8869	0.4996	0.8030	0.5238	0.7143	0.5334
0.2	1.3848	0.0001	1.3752	0.1050	1.3473	0.2054	1.3023	0.2997	1.2409	0.3832	1.1660	0.4532	1.0796	0.5092	0.9843	0.5477	0.8831	0.5699	0.7781	0.5743
0.3	1.6800	0.0003	1.6670	0.1221	1.6285	0.2406	1.5658	0.3495	1.4825	0.4444	1.3813	0.5222	1.2667	0.5816	1.1426	0.6192	1.0130	0.6389	0.8817	0.6378
0.4	2.1345	0.0001	2.1153	0.1491	2.0585	0.2906	1.9671	0.4207	1.8472	0.5295	1.7040	0.6198	1.5451	0.6783	1.3764	0.7175	1.2048	0.7307	1.0351	0.7215
0.5	2.8515	0.0001	2.8204	0.1910	2.7302	0.3698	2.5874	0.5278	2.4012	0.6578	2.1864	0.7553	1.9540	0.8187	1.7163	0.8452	1.4819	0.8446	1.2571	0.8229
0.6	4.0670	0.0001	4.0120	0.2592	3.8514	0.4979	3.6030	0.7028	3.2888	0.8622	2.9357	0.9674	2.5697	1.0203	2.2126	1.0263	1.8794	0.9931	1.5771	0.9395
0.7	6.4055	0.0029	6.2892	0.3969	5.9565	0.7527	5.4555	1.0368	4.8462	1.2262	4.1914	1.3382	3.5508	1.3477	2.9648	1.2981	2.4603	1.1916	2.0397	1.0700
0.8	12.052	0.0030	11.722	0.7318	10.815	1.3426	9.5135	1.7827	8.0400	2.0167	6.5868	2.0699	5.2781	1.9784	4.1869	1.7737	3.3407	1.4981	2.7221	1.2261
0.9	34.868	0.0144	32.990	2.0926	28.236	3.5486	22.364	4.2654	16.834	4.2433	12.307	3.8878	8.8825	3.3304	6.4268	2.7143	4.7765	2.0479	3.7817	1.4158

SIFs values of the single edge-notched plate (γ=35º) with clamped BC

Slant angle	0		5		10		15		20		25		30		35		40		45	
a/W	K_I	K_{II}	K_I	K_{II}	K_I	K_{II}	K_I	K_{II}	K_I	K_{II}	K_I	K_{II}	K_I	K_{II}	K_I	K_{II}	K_I	K_{II}	K_I	K_{II}
0.1	1.1331	0.0001	1.1267	0.0877	1.1075	0.1730	1.0760	0.2530	1.0330	0.3256	0.9795	0.3884	0.9164	0.4399	0.8454	0.4788	0.7679	0.5034	0.6852	0.5140
0.2	1.1566	0.0001	1.1494	0.0916	1.1287	0.1794	1.0951	0.2624	1.0490	0.3366	0.9922	0.3999	0.9260	0.4517	0.8519	0.4888	0.7718	0.5121	0.6872	0.5199
0.3	1.1889	0.0002	1.1809	0.0982	1.1571	0.1935	1.1183	0.2815	1.0665	0.3589	1.0032	0.4233	0.9308	0.4737	0.8515	0.5074	0.7671	0.5273	0.6799	0.5308
0.4	1.2390	0.0001	1.2289	0.1125	1.1991	0.2194	1.1511	0.3172	1.0882	0.3993	1.0130	0.4671	0.9295	0.5121	0.8404	0.5424	0.7491	0.5538	0.6577	0.5489
0.5	1.3192	0.0000	1.3054	0.1360	1.2658	0.2633	1.2032	0.3753	1.1217	0.4669	1.0277	0.5351	0.9260	0.5790	0.8220	0.5974	0.7193	0.5957	0.6205	0.5782
0.6	1.4472	0.0000	1.4284	0.1703	1.3733	0.3275	1.2880	0.4619	1.1796	0.5665	1.0572	0.6370	0.9292	0.6742	0.8027	0.6806	0.6833	0.6605	0.5741	0.6225
0.7	1.6560	0.0007	1.6286	0.2239	1.5496	0.4270	1.4292	0.5932	1.2803	0.7108	1.1161	0.7841	0.9507	0.8062	0.7931	0.7937	0.6512	0.7478	0.5275	0.6823
0.8	2.0280	0.0005	1.9840	0.3135	1.8610	0.5882	1.6776	0.8013	1.4585	0.9383	1.2284	1.0008	1.0055	1.0001	0.8033	0.9498	0.6302	0.8631	0.4872	0.7608
0.9	2.8930	0.0007	2.7969	0.5228	2.5414	0.9447	2.1901	1.2256	1.8105	1.3510	1.4461	1.3657	1.1219	1.2942	0.8470	1.1744	0.6266	1.0190	0.4590	0.8515

SIFs values of the single edge-notched plate (γ=40º) with pinned BC

Slant angle	0		5		10		15		20		25		30		35		40		45	
a/W	K_I	K_{II}	K_I	K_{II}	K_I	K_{II}	K_I	K_{II}	K_I	K_{II}	K_I	K_{II}	K_I	K_{II}	K_I	K_{II}	K_I	K_{II}	K_I	K_{II}
0.1	1.2105	0.0001	1.2032	0.0980	1.1813	0.1929	1.1456	0.2817	1.0970	0.3616	1.0368	0.4303	0.9664	0.4855	0.8876	0.5263	0.8020	0.5510	0.7119	0.5593
0.2	1.3924	0.0002	1.3823	0.1109	1.3544	0.2180	1.3085	0.3172	1.2463	0.4053	1.1702	0.4791	1.0823	0.5372	0.9855	0.5775	0.8828	0.5995	0.7764	0.6033
0.3	1.6889	0.0000	1.6756	0.1301	1.6369	0.2545	1.5733	0.3693	1.4891	0.4695	1.3868	0.5520	1.2709	0.6131	1.1453	0.6539	1.0141	0.6725	0.8814	0.6712
0.4	2.1455	0.0001	2.1258	0.1562	2.0686	0.3071	1.9767	0.4447	1.8552	0.5596	1.7110	0.6543	1.5507	0.7177	1.3807	0.7586	1.2075	0.7722	1.0364	0.7607
0.5	2.8653	0.0002	2.8339	0.2048	2.7428	0.3925	2.5995	0.5585	2.4125	0.6959	2.1961	0.7993	1.9619	0.8659	1.7220	0.8970	1.4866	0.8951	1.2603	0.8702
0.6	4.0859	0.0002	4.0311	0.2742	3.8701	0.5296	3.6198	0.7503	3.3043	0.9157	2.9490	1.0269	2.5813	1.0821	2.2220	1.0893	1.8862	1.0569	1.5825	0.9950
0.7	6.4360	0.0001	6.3189	0.4149	5.9857	0.8087	5.4810	1.1104	4.8694	1.3146	4.2116	1.4255	3.5673	1.4443	2.9784	1.3828	2.4708	1.2694	2.0471	1.1404
0.8	12.117	0.0002	11.782	0.7838	10.869	1.4480	9.5621	1.9307	8.0811	2.1807	6.6194	2.2310	5.3046	2.1351	4.2065	1.9094	3.3547	1.6107	2.7327	1.3093
0.9	35.082	0.0035	33.195	2.2834	28.411	3.8660	22.487	4.6648	16.926	4.6124	12.372	4.2377	8.9285	3.6360	6.4598	2.9294	4.7977	2.2153	3.7968	1.5198

SIFs values of the single edge-notched plate (γ=40º) with clamped BC

Slant angle	0		5		10		15		20		25		30		35		40		45	
a/W	K_I	K_{II}	K_I	K_{II}	K_I	K_{II}	K_I	K_{II}	K_I	K_{II}	K_I	K_{II}	K_I	K_{II}	K_I	K_{II}	K_I	K_{II}	K_I	K_{II}
0.1	1.1396	0.0001	1.1331	0.0930	1.1134	0.1831	1.0813	0.2677	1.0373	0.3442	0.9826	0.4104	0.9183	0.4641	0.8459	0.5043	0.7666	0.5294	0.6826	0.5387
0.2	1.1632	0.0001	1.1556	0.0968	1.1348	0.1905	1.1004	0.2779	1.0534	0.3563	0.9955	0.4229	0.9277	0.4766	0.8521	0.5153	0.7705	0.5383	0.6843	0.5453
0.3	1.1959	0.0000	1.1876	0.1048	1.1635	0.2052	1.1238	0.2981	1.0711	0.3798	1.0065	0.4479	0.9328	0.4996	0.8518	0.5356	0.7658	0.5542	0.6768	0.5570
0.4	1.2468	0.0000	1.2363	0.1187	1.2059	0.2328	1.1572	0.3364	1.0928	0.4233	1.0163	0.4941	0.9311	0.5423	0.8404	0.5731	0.7472	0.5838	0.6540	0.5761
0.5	1.3281	0.0001	1.3141	0.1459	1.2736	0.2804	1.2100	0.3988	1.1270	0.4957	1.0312	0.5676	0.9275	0.6131	0.8212	0.6331	0.7167	0.6292	0.6162	0.6075

0.6	1.4585	0.0001	1.4394	0.1812	1.3833	0.3494	1.2961	0.4936	1.1859	0.6033	1.0611	0.6772	0.9308	0.7152	0.8019	0.7209	0.6800	0.6993	0.5693	0.6539
0.7	1.6720	0.0000	1.6439	0.2373	1.5634	0.4581	1.4401	0.6351	1.2881	0.7606	1.1209	0.8354	0.9521	0.8607	0.7920	0.8425	0.6477	0.7908	0.5220	0.7198
0.8	2.0547	0.0000	2.0090	0.3378	1.8824	0.6347	1.6941	0.8648	1.4697	1.0099	1.2343	1.0730	1.0070	1.0714	0.8015	1.0132	0.6259	0.9167	0.4823	0.8004
0.9	2.9476	0.0003	2.8481	0.5743	2.5830	1.0335	2.2189	1.3366	1.8281	1.4637	1.4542	1.4763	1.1232	1.3946	0.8451	1.2537	0.6217	1.0853	0.4546	0.8971

SIFs values of the single edge-notched plate (γ=45º) with pinned BC

Slant angle	0		5		10		15		20		25		30		35		40		45	
a/W	K_I	K_{II}	K_I	K_{II}	K_I	K_{II}	K_I	K_{II}	K_I	K_{II}	K_I	K_{II}	K_I	K_{II}	K_I	K_{II}	K_I	K_{II}	K_I	K_{II}
0.1	1.2188	0.0000	1.2113	0.1039	1.1889	0.2039	1.1525	0.2977	1.1030	0.3819	1.0412	0.4539	0.9693	0.5120	0.8885	0.5542	0.8013	0.5784	0.7093	0.5855
0.2	1.4016	0.0000	1.3918	0.1172	1.3630	0.2297	1.3162	0.3351	1.2529	0.4281	1.1756	0.5062	1.0862	0.5666	0.9879	0.6080	0.8832	0.6303	0.7749	0.6335
0.3	1.6998	0.0004	1.6865	0.1367	1.6470	0.2703	1.5827	0.3899	1.4972	0.4963	1.3936	0.5813	1.2761	0.6483	1.1488	0.6905	1.0161	0.7078	0.8815	0.7061
0.4	2.1585	0.0001	2.1387	0.1659	2.0809	0.3266	1.9882	0.4699	1.8657	0.5941	1.7202	0.6925	1.5581	0.7599	1.3863	0.8025	1.2117	0.8138	1.0387	0.8030
0.5	2.8826	0.0003	2.8508	0.2151	2.7597	0.4114	2.6149	0.5925	2.4265	0.7397	2.2084	0.8461	1.9728	0.9156	1.7311	0.9497	1.4930	0.9485	1.2649	0.9215
0.6	4.1104	0.0009	4.0552	0.2910	3.8931	0.5665	3.6412	0.7957	3.3244	0.9725	2.9670	1.0961	2.5962	1.1499	2.2343	1.1565	1.8963	1.1203	1.5895	1.0585
0.7	6.4764	0.0007	6.3584	0.4582	6.0232	0.8757	5.5157	1.1940	4.8988	1.4151	4.2389	1.5249	3.5896	1.5466	2.9954	1.4881	2.4841	1.3587	2.0574	1.2140
0.8	12.199	0.0001	11.861	0.8661	10.945	1.5768	9.6256	2.0962	8.1368	2.3560	6.6634	2.4302	5.3392	2.3013	4.2329	2.0568	3.3746	1.7222	2.7472	1.4015
0.9	35.340	0.0134	33.436	2.6333	28.618	4.3142	22.651	5.1892	17.046	5.0999	12.462	4.5908	8.9905	3.9434	6.5009	3.1952	4.8283	2.3957	3.8164	1.6367

SIFs values of the single edge-notched plate (γ=45º) with clamped BC

Slant angle	0		5		10		15		20		25		30		35		40		45	
a/W	K_I	K_{II}	K_I	K_{II}	K_I	K_{II}	K_I	K_{II}	K_I	K_{II}	K_I	K_{II}	K_I	K_{II}	K_I	K_{II}	K_I	K_{II}	K_I	K_{II}
0.1	1.1475	0.0000	1.1407	0.0986	1.1206	0.1936	1.0877	0.2830	1.0429	0.3635	0.9867	0.4329	0.9209	0.4894	0.8465	0.5309	0.7656	0.5555	0.6796	0.5636
0.2	1.1711	0.0000	1.1637	0.1024	1.1421	0.2010	1.1069	0.2939	1.0588	0.3765	0.9996	0.4470	0.9304	0.5026	0.8531	0.5422	0.7695	0.5653	0.6811	0.5714
0.3	1.2043	0.0003	1.1959	0.1105	1.1711	0.2183	1.1306	0.3154	1.0766	0.4022	1.0106	0.4723	0.9351	0.5284	0.8523	0.5650	0.7644	0.5821	0.6731	0.5836
0.4	1.2558	0.0001	1.2452	0.1264	1.2141	0.2482	1.1644	0.3567	1.0987	0.4501	1.0206	0.5237	0.9334	0.5742	0.8406	0.6054	0.7454	0.6136	0.6499	0.6044
0.5	1.3389	0.0001	1.3245	0.1543	1.2833	0.2962	1.2182	0.4243	1.1335	0.5276	1.0356	0.6018	0.9299	0.6485	0.8213	0.6689	0.7141	0.6636	0.6113	0.6381
0.6	1.4720	0.0003	1.4524	0.1931	1.3951	0.3738	1.3060	0.5253	1.1935	0.6418	1.0662	0.7215	0.9330	0.7591	0.8015	0.7630	0.6772	0.7368	0.5640	0.6884
0.7	1.6911	0.0002	1.6622	0.2579	1.5796	0.4934	1.4534	0.6811	1.2975	0.8157	1.1271	0.8911	0.9546	0.9169	0.7909	0.8974	0.6442	0.8379	0.5171	0.7559
0.8	2.0857	0.0000	2.0384	0.3685	1.9081	0.6875	1.7136	0.9340	1.4834	1.0858	1.2418	1.1558	1.0099	1.1449	0.8006	1.0782	0.6228	0.9688	0.4783	0.8424
0.9	3.0104	0.0007	2.9061	0.6436	2.6300	1.1429	2.2521	1.4700	1.8483	1.5979	1.4653	1.5900	1.1267	1.4964	0.8436	1.3421	0.6191	1.1505	0.4519	0.9458